2015

THERMODYNAMICS OF HHR23A UBIQUITIN-ASSOCIATED (UBA) DOMAINS

Moses Joseph Leavens
University of Montana, Missoula

THERMODYNAMICS OF HHR23A UBIQUITIN-ASSOCIATED (UBA) DOMAINS

By

Moses Joseph Leavens

A.S., General Education, Montana State University College of Technology, Great Falls, MT, USA, 2006

B.A. Biology & Chemistry, B.S. Mathematics, University of Great Falls, Great Falls, MT, USA, 2011

Thesis

Presented in partial fulfillment of the requirements
For the degree of

Master of Science
In Biochemistry & Biophysics

The University of Montana
Missoula, MT

December 2015

Approved by:

Dr. J.B. Alexander (Sandy) Ross, Dean of the Graduate School
Graduate School

Dr. Bruce E. Bowler, Committee Chairperson
Department of Chemistry & Biochemistry

Dr. Steve Lodmell, Committee Member
Division of Biological Sciences

Dr. J.B. Alexander (Sandy) Ross, Committee Member
Department of Chemistry & Biochemistry

Dr. Stephen Sprang, Committee Member
Division of Biological Sciences

Dr. Scott Wetzel, Committee Member
Division of Biological Sciences

Leavens, Moses J., M.S., Fall 2015 Chemistry & Biochemistry

Thermodynamics of HHR23A Ubiquitin-associated (UBA) domains

Chairperson: Bruce E. Bowler

Ubiquitin-associated (UBA) domains have been discovered in several proteins within the cell, and at least one domain plays an important functional role in cellular phenomena such as NF-κB signaling. Mutations within the UBA(2) domain of the ubiquitin-binding scaffold protein p62 are frequently observed in patients suffering from Paget's disease of bone. The human DNA excision repair protein HHR23A contains the UBA(1) and UBA(2) domains, and nuclear magnetic resonance (NMR) structures depict their compact three-helix bundles. Moreover, the HHR23A UBA(1) and UBA(2) only share approximately 20% primary sequence identity. The p62 UBA(2) domain has been shown to contain quaternary structure in the μM concentration range, and has been hypothesized to play an important functional role within the cell via ubiquitination. Herein, the HHR23A UBA domain thermodynamics are determined using far UV CD guanidine hydrochloride titrations, and a UBA(1) quaternary structure investigation is carried out using matrix-assisted laser desorption/ionization mass spectrometry, far UV CD thermal denaturation, and gel filtration size exclusion chromatography (SEC) to elucidate a possible shared property between the p62 and HHR23A UBA domains, which may suggest potential competition between ubiquitin binding and UBA domain dimerization. Our results demonstrate that a C26A mutation in the UBA(2) domain enhances its stability, and that no change in the UBA(1) equilibrium constant for unfolding is observed as a function of protein concentration, indicating no HHR23A UBA(1) dimerization in the uM concentration range. Furthermore, the HHR23A UBA(1) domain interacts with ubiquitin, yet these HHR23A UBA domains do not interact with each other, indicating a different mechanism other than HHR23A UBA domain homodimerization is involved.

Acknowledgements

None of my work would have been possible without the help of the Bruce Bowler lab for their training. Thus, I would like to acknowledge Bruce and members of our lab for guidance and training me on this project. In addition, I would like to thank Aaron Thomas and the Sloan Indigenous Graduate Partnership for Aaron's mentorship, and to the Sloan Foundation, for supporting me through my graduate education.

I would like to acknowledge my grandfather and high school running coach, who taught me the importance of hard work, determination, resiliency, and perseverance. I am especially grateful for family and friends who have inspired me to change and go above and beyond—not to compete with others, but to better myself so I could help. To Raina and Zoey, who have sacrificed their time so I could accomplish my lab work.

I am undoubtedly indebted to helping others, for the people aforementioned who have helped me through life.

Now, "let us follow the truth, whither so ever it leads" - Socrates

Table of Contents

List of Figures

List of Tables

List of Equations

Chapter 1: Introduction

Proteins are fundamental to carrying out life processes. From cell communication—regulation of the cell cycle by way of cyclins, to the immune system—antibodies recognizing a distinct epitope to neutralize an immunogen, proteins are the essence of an organism's living template. Made up of amino acids, these biological macromolecules are folded into a three dimensional structure that aids a protein to carry out its function. At one time, it was thought that a protein could only fold into a compact, native structure, and give rise to a single function. However, with advances in protein folding research, we now understand that proteins are not static, but dynamic, in that proteins fluctuate from one conformation to another to give rise to their functional versatility. There are several examples of this in nature, and an intriguing example of this observation is the Ubiquitin-associated (UBA) domains, which is described herein.

Many proteins fold from their primary sequence to a tertiary structure with no assistance. At one time, it was thought that the environment of a living cell was required to assist a protein to fold into its three dimensional structure; however, this has not been the case with many proteins, as proteins do fold independently. Many of these proteins that fold independently do not contain covalent cross-linkages or disulfide bonds. One of the pioneers in protein folding research is Christian Anfinsen. Anfinsen and his colleagues investigated this question—whether a protein can renature to its native conformation and also retain activity using ribonuclease A as a model system. They discovered that upon denaturing ribonuclease in 8 M urea containing 2-mercaptoethanol, and then restoring the oxidizing and physiological conditions, that ribonuclease can return to its native conformation and have activity that is indistinguishable from the native ribonuclease molecule (Anfinsen, 1973).

Anfinsen's work led to the formulation of the thermodynamic hypothesis. The hypothesis states that small globular proteins rely only on their primary sequence to fold to their native three dimensional structures (Anfinsen, 1973). Or more thermodynamically stated that a protein in its native conformation under physiological conditions is the conformation that is the most energetically favorable. The hypothesis is governed by additional conditions: the native structure is readily accessible (no intermediate barriers) and is unique—in that the primary sequence encodes only one conformation.

Moreover, altered thermodynamic states of proteins have been discovered that have less favorable free energies than the native state. These alterations from a native state reveal protein dynamics that contribute to diseases of higher order organisms. The conformational states of these proteins have popularly been termed 'misfolded' or the 'denatured state ensemble,' and play a key role in common diseases such as Alzheimer's, Parkinson's, Paget's disease of bone, and bovine spongiform encephalopathy. Interestingly, the free energy change between a protein's native conformation and a denatured state is approximately between 5-15 kcal/mole.

There are several factors that can alter a protein's native structure. Mutations occurring in an individual's genome within the coding region can cause a particular protein to be misfolded from its native state. A well-known example is the disease Cystic Fibrosis, where mutations in the *CFTR* gene cause an alteration in this protein that helps control the balance of salt and water within the cell. An individual's environment, such as diet, may also play a role in affecting protein dynamics, as misfolded proteins can contribute to oxidative stress within the cell, and produce abnormal levels of reduced oxygen species and reduced nitrogen species, which contribute to tissue degeneration (Gregersen N, 2010).

Ubiquitin-associated domains are no exception to this phenomenon of protein unfolding. The Ubiquitin scaffolding protein p62 containing specific mutations within its UBA domain, leads to disruptions in ubiquitin signaling and is a molecular signature of Paget's disease of bone (Jed Long, 2010). Moreover, these UBA domains are widespread throughout several families of proteins. From the protein kinases to ubiquitin scaffolding proteins to nucleotide excision repair proteins, these small domains are pervasive. More importantly, because UBA domains are only approximately 50 amino acids and contain no covalent cross-linkages or disulfide bonds, they provide an excellent model system for protein folding studies.

Interestingly, a GST pulldown assay shows that the p62 UBA domain forms dimers *in vivo* (Jed Long, 2010). Moreover, far UV circular dichroism spectroscopy heat denaturation experiments using different concentrations of the p62 UBA domain reveal a shift in the melting temperature of this domain, indicating quaternary structure occurring at micromolar concentrations. Observations of this p62 UBA domain stability shift occurred around 10 uM protein concentration. Furthermore, isothermal titration calorimetry and fluorescence kinetic studies indicate that the equilibrium dissociation constant for the p62 UBA domain at 25 ˚C is 4-12 uM, depending on which method was employed.

Subsequent X-ray crystallography experiments with the mouse p62 UBA domain shows that the resolved structure is dimeric with C2 axial symmetry. In addition, an NMR titration experiment with mouse p62 UBA domain and ubiquitin indicate that the UBA domain binding site for ubiquitin partially overlaps with the binding site for homodimer formation (Shin Isogai, 2011). One model for the interaction of ubiquitin with the p62 UBA domain suggests that the p62 UBA domain dimerization is the 'off state' for ubiquitin signaling. Interestingly, once

ubiquitin binds to a p62 UBA domain monomer, this dimer interaction is released; making the monomeric state the 'on state' for this p62 UBA domain.

Because of the widespread nature of UBA domains in proteins and the phenomenon of quaternary structure in some UBA domains *in vitro* and *in vivo*, it was a goal of our protein folding studies to determine whether quaternary structure is occurring with the internal UBA domain of the human DNA excision-repair protein HHR23A. Furthermore, the Gibbs free energy of unfolding will be measured for HHR23A UBA domain variants, as well as other UBA(1) domain thermodynamic parameters, to help us understand the thermodynamic properties of these three helix bundles (Fig.1.1).

Therefore, the goal of this research project is two-fold: determine the thermodynamic stabilities of the HHR23A UBA domains, and to ascertain whether the HHR23A UBA(1) domain forms quaternary structure. To determine the thermodynamics of these HHR23A UBA domains, they will be subjected to a guanidine hydrochloride titration melt using far UV circular dichroism spectroscopy to monitor secondary structure, where the thermodynamics of these UBA domains will be measured using a two state protein folding model. In addition, a thermal denaturation study will be carried out for the HHR23A UBA(1) domain to determine whether or not a shift in temperature at the midpoint of the folding transition (T_m) occurs at different concentrations. Substantial differences in the melting temperature values would suggest dimerization, as demonstrated in the p62 UBA domain (Jed Long, 2010). Moreover, the Gibbs free energy of unfolding for the UBA(1) domain at 298.15 K will be compared using the two different denaturation methods. Fast protein liquid chromatography size exclusion chromatography and native polyacrylamide gel electrophoresis will also be employed to supplement the thermal denaturation dimerization experiment.

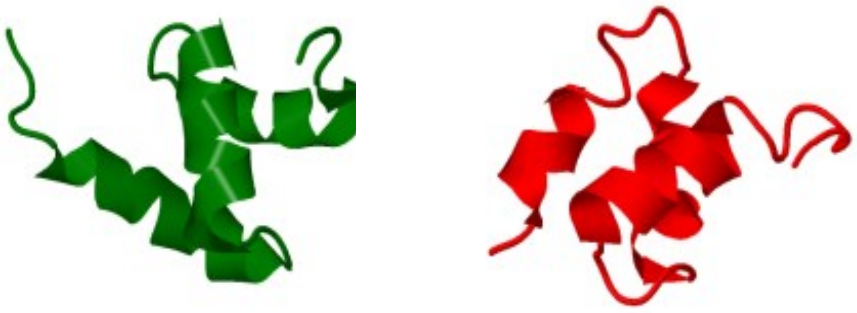

UBA(1): TLVTGSEYETMLTEIMSMGYERERVVAALRASYNNPHRAVEYLLTGIPG

UBA(2): QEKEAIERLKALGFPESLVIQAYFACEKNENLAANFLLSQNFDDE

Fig. 1.1. NMR solution structures of the human DNA excision repair protein HHR23A UBA(1) domain (left, PDB 1IFY) and C-terminal UBA(2) domain (right, PDB 1DV0). The amino acid sequences of HHR23A UBA(1) and UBA(2) domain are displayed, where underlines indicate the secondary structure.

Chapter 2: Materials & Methodology

2A: Growth, Isolation, and Purification of Ubiquitin-Associated Domains

Plasmids encoding the cDNA sequences of each of two Ubiquitin-associated (UBA) domains were transformed into BL21 (DE3) *Escherichia coli* competent cells - the UBA(1) domain and the UBA(2) domain. Two pGEX-2T plasmids, one containing the UBA(1) sequence and the other plasmid containing the UBA(2) domain sequence, were supplied by Juli Feigon et al. (Thomas D. Mueller, 2002). The pGEX-2T plasmid is 4,948 base pairs and contains the following elements: a glutathione S-transferase (GST) gene region, a multiple cloning site, a β-lactamase gene region, a *lac*I_q nucleotide region, an origin of replication site, and nucleotide binding sites for the 5' and 3' pGEX sequencing primers (pGEX-2T vector map, GE Healthcare).

Additionally, the glutathione S-transferase gene region contains the following: a *tac* promoter, a *lac* operator, a ribosome binding site for GST, and a coding sequence for a biotinylated thrombin to cleave the GST tag from the UBA domain. The amino acid sequence of the UBA(1) domain was discovered as an internal domain of the human DNA excision repair protein HHR23A, while the UBA(2) domain sequence is located at the C-terminal end of HHR23A. The protein HHR23A is a homolog of the *Saccharomyces cerevisiae* RAD23 protein, which is also a DNA excision repair protein.

To grow these UBA domains, their plasmid DNA at concentrations of approximately 100 ng/ul were added at 0.6 ul volume to 5 ul of BL21 (DE3) *Escherichia coli* competent cells using a P-10 pipet and 1.7 ml sterile Eppendorf tubes. The cells were immediately placed on ice to allow for the plasmid DNA to adhere to the *Escherichia coli* plasma membrane. After 45 minutes, the cells were heat shocked in a water bath at 42 ˚C for 45 seconds to permeabilize the plasma membrane—allowing the plasmid DNA to enter the cell. After 45 seconds, the samples were immediately placed back on ice for 5 minutes to close the bacterial membrane.

Subsequently, 1 ml of sterile L-broth (10 g tryptone, 6 g NaCl, 5 g yeast extract in 1 L MilliQ H_2O) media was added to these transformed cells, mixed, and shaken at 100 rpm at 37 ˚C for 1.5 hours to allow growth of the transformed *Escherichia coli* cells and expression of ampicillin resistance. After 1.5 hours, these cells were then inoculated onto freshly made L-ampicillin plates (5 g tryptone, 2.5 g yeast extract, 3 g NaCl, 7.5 g agar in 0.5 L MilliQ H_2O, 0.5 ml of 100 mg/ml sterile L-ampicillin) at either 50 ul or 100 ul volumes using sterile technique. These plates were subsequently incubated at 37 ˚C for 16-18 hours to obtain distinct transformed colonies. Typically, 50 ul of growth media was sufficient to obtain a high density of colonies for either UBA domain vector.

After this period of time, one distinct colony was selected with a sterile toothpick using 95% ethanol flamed tweezers and subsequently transferred into sterile 125 ml Erlenmeyer flasks containing 10 ml of sterile L-broth and 10 ul of 100 mg/ml L-ampicillin to commence growth of the mini-culture. These mini-cultures were then incubated at 37 ˚C at 100 rpm overnight for approximately 21 hours. After this period of time, the 10 ml mini-cultures were removed from the 37 ˚C shaker and using a sterile 10 ml pipet, were inoculated into 1 L of sterilized L-broth containing 1 ml of 100 mg/ml L-ampicillin. The 1 L flasks were placed in a 37 ˚C shaker at 150 rpm and monitored for their growth using optical density at 550 nm (OD_{550}). The OD_{550} was measured using 3 ml x 1 cm cuvettes and a Beckmann Coulter UV-Vis spectrophotometer.

When the OD_{550} was equal to 0.7, each 1 L culture was inoculated with 1 M of syringe filtered (0.2 micron sterile filter) isopropyl-beta-D-thiogalactoside (IPTG) to a final IPTG concentration equal to 1 mM. Typically, the total time to reach $OD_{550} = 0.7$ was approximately 3 hours, dependent on the total amount of time the 10 ml mini-cultures had grown. After inoculation with IPTG, the 1 L cultures were incubated at 30˚C for 3 hours and shaken at 125

rpm during this time. After 3 hours, the culture was poured into balanced Nalgene plastic centrifuge bottles and spun at 5,000 rpm for 10 minute cycles using a Thermo-scientific centrifuge with an F12 rotor. Bottles were weighed with their caps prior to filling with liquid to obtain an initial mass. After pelleted cells were obtained, the supernatant was poured off into empty Fernbach flasks and subsequently autoclaved for waste. The pelleted cells were then weighed with their caps and the final mass minus the initial mass was recorded to obtain cell pellet mass. After cell masses were recorded for each bottle, the bottles were either frozen at -80 ˚C for storage or lysed immediately. For cell lysis, the detergent Bugbuster (EMD Millipore) was used. For every gram of cells, 5 ml of Bugbuster detergent was added to the cell pellet. The total volume of detergent was added to one bottle, mixed using a 25 ml sterile pipet, and then the cell lysis solution was transferred to the next bottle of cells until all lysed cells were combined into one Nalgene bottle.

When the cells were combined into one Nalgene bottle, the enzyme benzonase nuclease was added. For each ml of Bugbuster detergent, one ul of benzonase nuclease was added to the pooled cell lysis solution. For a 1 L protein prep, typically 30 ml of detergent was used for cell lysis thus 30 ul of benzonase nuclease was added to the solution. Subsequently, the bottle containing all lysed cells was put on a room temperature shaker at 75 rpm for 20 minutes to ensure efficient nucleic acid degradation and to get the UBA-GST fusion proteins into solution. After this time, the lysed cells were spun down in a Thermo-scientific centrifuge with an F14 rotor for 20 minutes, 4˚C, and at 11,600 rpm.

The supernatant was harvested and added directly to a prepared Glutathione-S-transferase affinity column. The GST affinity column contains a GST bind resin for quick purification of recombinant GST fusion proteins. The GST domain is 220 amino acids, and can be eluted using

10 mM reduced glutathione (EMD Millipore). Additionally, the GST bind resin uses a 14 atom spacer arm that is approximately 22 Angstroms for covalent attachment of reduced glutathione using a disulfide linkage (EMD Millipore). The GST bind kit comes pre-packaged from EMD Millipore, where the kit contains 10 ml GST bind resin, 200 ml of 10X GST bind/wash buffer (43 mM Na_2HPO_4, 1.37 M NaCl, 14.7 mM KH_2PO_4, 27 mM KCl, pH 7.2 ± 0.2), 40 ml of 10X Glutathione reconstitution buffer (500 mM Tris-HCl, pH 8.0), and 1 g of reduced, free acid glutathione. To be cost effective, the 10X GST bind/wash buffer and the 10X GST elution buffer were made in house and subsequently used for these UBA domain preps.

The 10 ml GST bind resin is stored in 20% ethanol when not in use, and to prepare the GST affinity column, the resin is mixed then added to a 20 ml x 1 cm diameter column. Once the GST resin is settled, the ethanol is removed using a transfer pipet. The resin is then washed with 50 ml of 1X GST bind/wash buffer and then is ready to accept supernatant from the cell lysis solution. After about 3 ml of supernatant is added directly to the column, the remaining ~27 mL of supernatant is run into the column using gravity flow from a reservoir and connected capillary tube that rests above the column. The supernatant flows through the column allowing for GST-UBA fusion protein capture. Once the supernatant flows through, the GST column is washed with 100 ml of 1X GST bind/wash buffer. The first 4 wash fractions are collected in 7 ml volumes using 15 ml falcon tubes, and then a large 50 ml falcon tube is used to collect the rest of the wash buffer.

After washing, a 30 ml 1X GST elution buffer is added to the column to allow for the GST and the reduced glutathione to bind, which subsequently releases the captured GST-UBA fusion protein. The column eluates are collected in 7 ml volumes using 15 ml falcon tubes until all 30 ml of elution buffer is collected from the column. The column is then washed with 50 ml of 1X

GST bind/wash buffer and subsequently stored back in 20% ethanol for future use. The first 4 - 7 ml wash fractions and all the elution fractions are then measured for their absorbance at 280 nm using a 1 cm path length and a Beckmann Coulter UV-Vis spectrophotometer. Usually eluate 2 and eluate 3 contain the GST-UBA fusion protein.

These elution fractions containing the GST-UBA fusion protein are collected and then concentrated by centrifuge ultrafiltration using either a 5,000 or 3,000 molecular weight cut off (MWCO) membrane. Usually, a 15 ml 3,000 MWCO concentrator works best because of longer spinning durations. The fractions are loaded into the equilibrated concentrator, and then spun at 3,200 rpm until all fractions containing GST-UBA fusion protein are concentrated down to approximately 1 ml volume. Once the fractions are concentrated to 1 ml, the solution is buffer exchanged into a 1X thrombin cleavage buffer (10 mM Tris, 0.15 M NaCl, 2.5 mM $CaCl_2$, pH 8.0) to 12 times the volume of the concentrated protein to ensure the protein is entirely into the 1X thrombin cleavage buffer.

When the GST-UBA fusion construct is concentrated to approximately 1.5 ml in 1X thrombin cleavage buffer, the absorbance at 280 nm is measured using a 1 cm path length. Because the protein is highly concentrated, a 1:30 dilution is prepared and then its absorbance is measured. The extinction coefficient for UBA(1) domain is 5,690 $M^{-1}cm^{-1}$ at 280 nm, while the extinction coefficient for UBA(2) domain is 1,490 $M^{-1}cm^{-1}$ at 280 nm. However, because GST is covalently bound to the UBA domain, we cannot use these extinction coefficients. Therefore, we use the result that when GST's $A_{280} = 1$ its concentration is equal to 0.5 mg/ml. In this way, we can use the mathematical relationship $1/0.5 = A_{280}/X$. We know the A_{280} for GST-UBA, so we just need to multiply by 0.5 to get our GST-UBA protein concentration in mg/ml.

We take our concentration in mg/ml and multiply by the total volume of our solution to obtain the milligrams of our GST-UBA fusion protein. Because GST is 220 amino acids and UBA(1) and UBA(2) are 51 and 43 amino acids, respectively, our UBA domain will be approximately 20% of the primary sequence of the GST-UBA fusion protein. Therefore, we multiply 0.2 by the total amount of protein in milligrams to obtain the milligrams of UBA domain. Usually for a 1 L prep, about 5 mg of UBA domain is typically obtained.

Biotinylated thrombin is used to cut between an arginine and glycine sequence upstream of the UBA domain primary sequence. The biotinylated thrombin comes pre-packaged from EMD Millipore, and it is usually at a concentration of 0.6 U per microliter. Because 1 U is required to cleave 1 mg of GST-UBA fusion protein, we set up a conversion to ascertain how much enzyme to add to our GST-UBA fusion protein. We factor in the amount of GST also, so we take our total number of milligrams of GST-UBA protein and divide by 0.6 to determine the microliter volume of enzyme to add to the protein solution. Once the enzyme is added to the protein in a 15 ml sterile falcon tube, it is placed at room temperature on a shaker for 16-18 hours for efficient cleavage of GST tag. For the UBA(1) domain, the biotinylated thrombin recognizes the RG primary sequence located 8 amino acids upstream of the first amino acid residue in the UBA(1) primary sequence.

After cleavage, the biotinylated thrombin is removed using streptavidin agarose (EMD Millipore). Because of the high avidity for biotin and streptavidin, the thrombin can be captured using 2 ml spin filters. In brief, the cleaved UBA domain, GST, and biotinylated thrombin solution is pipetted onto the filter and centrifuged at room temperature for 5 minutes at 2,500 rpm. The streptavidin agarose-biotinylated thrombin will be retained on the filter while the cleaved UBA domain with free GST passes through the filter. This solution is then added onto a

second GST affinity column. This protein solution passes through the GST bind resin where the flow through is collected in a 15 ml falcon tube.

After the protein solution passes through the column, the column is washed with 100 ml of 1X GST bind/wash buffer. The wash fractions are collected in 7 ml fractions using sterile 15 ml falcon tubes. Subsequently, GST is eluted from the column using 1X GST elution buffer. These GST fractions are usually kept as a standard for sodium dodecyl sulfate polyacrylamide gel electrophoresis (SDS-PAGE) experiments. The A_{280} of these fractions are checked using a Beckmann-Coulter UV-Vis spectrophotometer, and wash fractions containing cut UBA domain are concentrated in a 15 ml 3,000 MWCO ultracentrifugation device at 4 ˚C until the protein solution is approximately 1 ml.

Once the protein is concentrated to 1 ml, it is buffer exchanged into a UBA pH 6.5 buffer (100 mM NaCl, 50 mM Na_2HPO_4) 12 times to ensure protein is completely in this new buffer. Final purification of the UBA(1) domain was initially carried out using a high performance liquid chromatography (HPLC) ion-exchange column, but the UBA(1) domain did not adhere well to this column. Subsequently, we discovered size-exclusion chromatography worked well as a final purification step for both the HHR23A UBA(1) and the UBA(2) domains, as we discovered that residual GST is present after cleavage methodology. The column used for fast protein liquid chromatography (FPLC) gel filtration size-exclusion chromatography is a Superdex 300/10 GL column (GE Healthcare) and is efficient for separation of small peptides. The ideal ranges for separation using this column are molecules that are between 100-7000 Daltons. Because UBA(1) is 5,635.3 g/mol, and UBA(2) is 5,259.81 g/mol, this column was ideal for separating these domains from residual GST.

2B: FPLC – Size Exclusion Chromatography

The Superdex Peptide 10/300 GL high performance column is a glass column for high performance gel filtration of natural, recombinant, or synthetic peptides and other small biomolecules (GE Healthcare Superdex Peptide 10/300 GL manual). One column volume for the Superdex 10/300 GL column is approximately 24 ml. Following GE Healthcare Life Sciences manual guidelines, the column is stored in 20% ethanol and washed using filtered MilliQ H_2O at a flow rate of 0.2 ml/min for approximately 50 milliliters. After the water washing step, the column is flushed with at least 2 column volumes of UBA pH 6.5 buffer at a flow rate of 0.4 ml/min. The column is cleaned after 10 protein purifications using 0.5 M NaOH at a flow rate of 0.4 ml/min for 1 column volume, and then immediately flushed with 2 column volumes of filtered MilliQ H_2O at a flow rate of 0.2 ml/min.

To prepare the protein for size-exclusion chromatography experiments, a final purification was first carried out individually for the UBA(1) and the UBA(2) C26A domain (Fig 2.1). The UBA domains were concentrated to approximately 1 ml and buffer exchanged 12-fold using the UBA pH 6.5 buffer solution (100 mM NaCl, 50 mM Na_2HPO_4). The proteins were then subsequently loaded individually onto the size-exclusion column using a clean 1 ml plastic syringe. The 0.5 ml fractions that contained the monomer (according to the equine cytochrome *c* standard, Fig 3.3) were collected, pooled, and then concentrated for further use. For bovine ubiquitin, its molecular weight is 8,560 g/mol (pI = 6.6) and comes packaged pure in a lyophilized powder supplied by Sigma Aldrich. The extinction coefficient and isoelectric point of ubiquitin was determined using ExPasy, and because no tryptophan is present in ubiquitin's primary sequence, the extinction coefficient was calculated to be 1,490 $M^{-1}cm^{-1}$.

For the UBA(1) and bovine ubiquitin experiment, both proteins were prepared in the UBA pH 6.5 buffer. After collection from the size exclusion column and being concentrated briefly using a 3,000 MWCO concentrator, the peptide stock solutions A_{280} was measured using a 1 cm cuvette on a Beckmann Coulter UV-Vis spectrophotometer. Dilutions were then made to 100 uM at 1 ml volume using sterile 1.7 ml Eppendorf tubes and then their concentrations were confirmed using the UV-Vis spectrophotometer. The UBA(1) and ubiquitin samples were then mixed 1:1 using 0.5 ml of 100 uM UBA(1) domain and 0.5 ml of 100 uM ubiquitin for 5 minutes at room temperature. At approximately 5 minute mixing time, 1 ml was taken up from this peptide mixture using a clean 1 ml plastic syringe and loaded onto the column at 4 ˚C.

For the UBA(2) C26A and ubiquitin experiments, similar conditions were applied. Both the UBA(2) C26A domain and bovine ubiquitin were purified via the size exclusion column using a UBA pH 6.5 buffer. Because the stock bovine ubiquitin solution sat for 4 days at 4˚C, it needed to be purified via size exclusion chromatography before testing its interaction with UBA(2) C26A domain. After pooling and brief concentration of these 0.5 ml fractions, their protein stock solutions A_{280} were measured using a 1 cm cuvette on a Beckmann Coulter UV-Vis spectrophotometer. Dilutions were made to 100 uM and then were confirmed using the UV-Vis spectrophotometer. The UBA(2) C26A domain and ubiquitin 100 uM solutions were then mixed 1:1 ratio volume (400 ul for each solution) for a total volume of 800 ul. After 25 minute incubation at ambient temperature, approximately 800 ul was taken up from this peptide mixture using a clean 1 ml plastic syringe and loaded onto the column at 4 ˚C.

Bovine ubiquitin was also used a standard to assess whether these HHR23A UBA domains elute off the column as a monomer or dimer (ubiquitin data not shown because equine cytochrome *c* provided a molecular weight close to dimer for either domain, ~12.384 kD). In this

way, equine heart cytochrome *c* (pI = 10-10.5) was prepared in UBA pH 6.5 buffer and its concentration was measured using a Beckmann Coulter UV-Vis spectrophotometer. Five absorbance values at 550 nm (9.0 x 10^3 M^{-1} cm^{-1}), 541.8 nm (9.0 x 10^3 M^{-1} cm^{-1}), 526.5 nm (11.0 x 10^3 M^{-1} cm^{-1}), 360 nm (28.5 x 10^3 M^{-1} cm^{-1}), and 339 nm (20.9 x 10^3 M^{-1} cm^{-1}) were used to calculate the stock concentration for cytochrome c, which was determined to be 600 uM (Margoliash, E.; Frohwirt, Nehamah;, 1959).

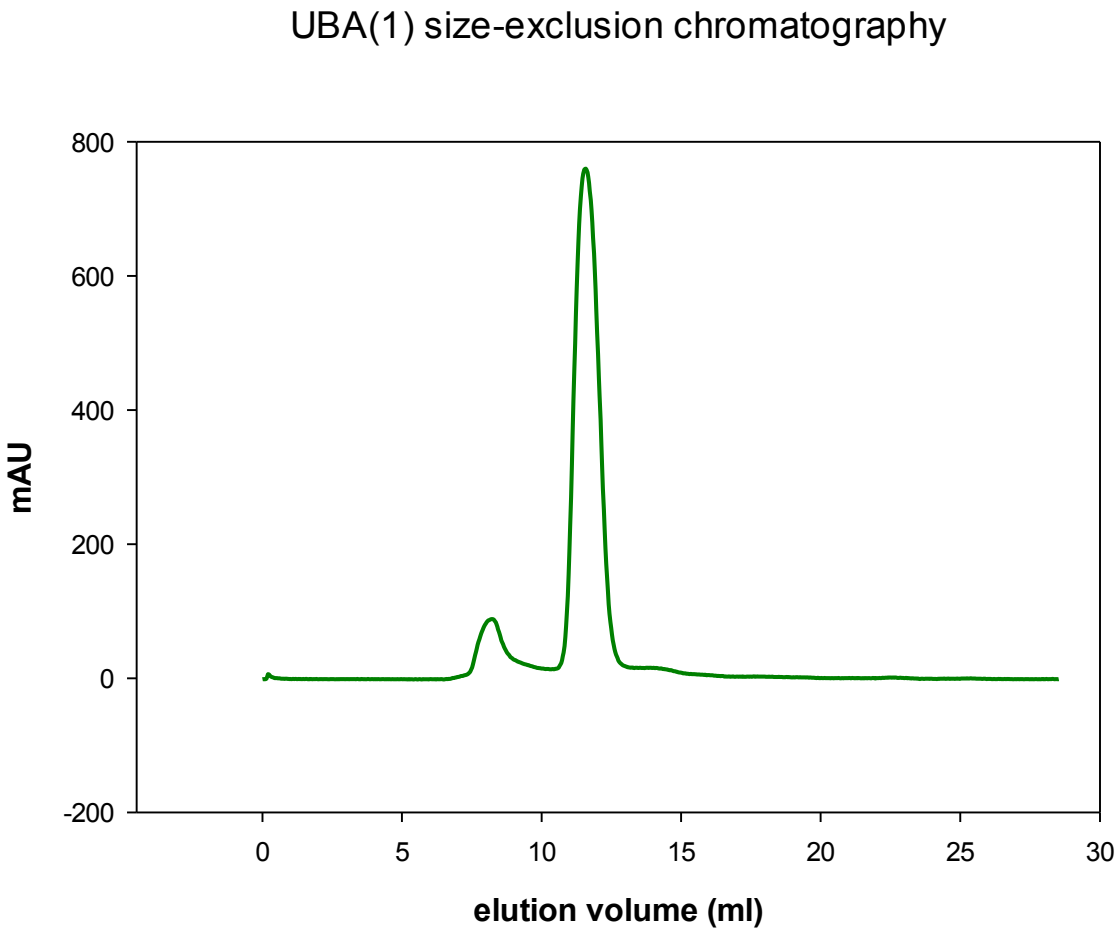

Fig. 2.1. Standard FPLC size exclusion chromatogram of the HHR23A UBA(1) domain from final purification. Concentration prior to loading onto column was 600 uM.

2C: Sodium Dodecyl Sulfate Polyacrylamide Gel Electrophoresis (SDS-PAGE)

Conditions for SDS-PAGE were carried out with a 1X Tris-glycine buffer (24.7 mM Tris, 191.8 mM glycine, 3.46 mM SDS, pH 8.5) using Mini-PROTEAN TGX Precast gels (Bio-Rad). After the samples (except GST-UBA(1)) were subjected to a second GST affinity column, they were collected and concentrated using a 3,500 MWCO membrane to approximately 1.5 ml and then checked for their A_{280} using a 1 cm path length on a Beckmann Coulter UV-Vis spectrophotometer. After the GST, GST-UBA(1), UBA(1), UBA(2) absorbances were determined, their concentrations were calculated using their respective extinction coefficients (see Section 2A). All sample concentrations were calculated in micrograms per microliter, and a 5 ug mass was used to determine the gel load volume.

After the gel load volume was determined, the volume of each sample was pipetted into an individual sterile 1.7 ml Eppendorf tube. The reagent β-mercaptoethanol was added to each sample at 0.5 ul, and subsequently, gel loading dye was added where its volume equaled the volume of sample added. All samples contained approximately equal volumes, were spun briefly, and placed in a boiling water bath for 5 minutes. After the boiling step, the samples were again briefly spun, and 10 ul of volume was loaded into each lane. A Bio-Rad precision plus gel loading protein standard was added at a volume of 10 ul to determine molecular weights of the samples. The gel was run for approximately 1 hour at 80 V. After the gel loading dye had migrated further than the 10 kD protein standard, the voltage was discontinued. The gel was removed from the apparatus and washed with MilliQ H_2O for 30 minutes. Subsequently, Coomassie brilliant blue stain was added to the gel and stained for 2 hours. After staining, a destain solution (10% ethanol and 40% glacial acetic acid) was applied for 2 hours with gentle

mixing at room temperature. The bands were visualized with white light to determine each sample's molecular weight and purity (Fig 2.2).

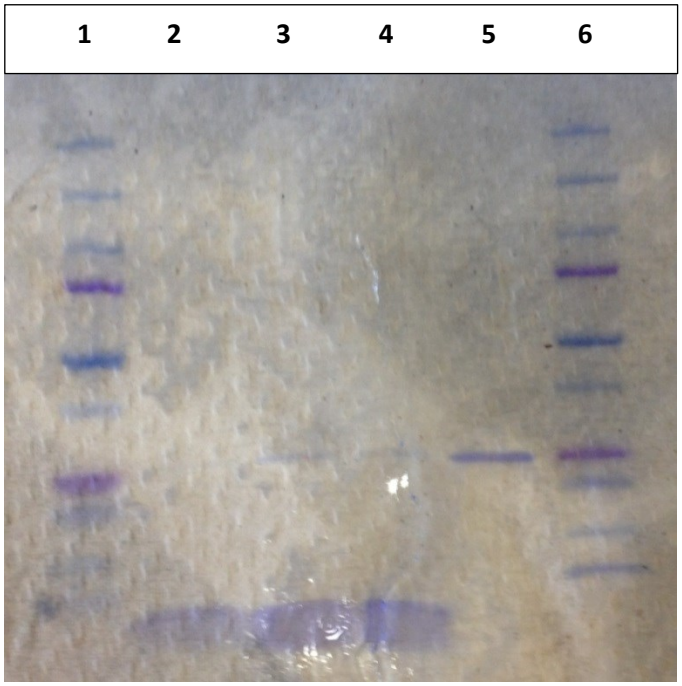

Fig. 2.2. SDS-PAGE of the UBA(1) domain before final purification. Lanes 2,3, and 4 are 5.6 kD UBA(1) domain fractions after second GST affinity column, showing residual GST, while lane 5 is 26 kD cleaved GST. Lanes 1 and 6 are Bio-Rad precision plus MW standards.

2D: Native Polyacrylamide Gel Electrophoresis (Native PAGE)

For native gel electrophoresis, the UBA pH 6.5 buffer (100 mM NaCl, 50 mM $NaH_2PO_4 \cdot H_2O$) was used for all samples except insulin. Insulin had solubility issues around neutral pH, so the UBA pH 8 buffer was used. The UBA(1) domain was purified through a Superdex Peptide 10/300 GL column via size-exclusion chromatography, where a peak at approximately 25 kD containing a small absorbance at 280 nm was isolated (Fig 2.1). The 0.5 ml eluent fractions for this large peak were collected for subsequent analysis and discovered to be residual glutathione S-transferase (Fig 3.7). Moreover, a lower molecular weight peak of 5.6 kD with a large absorbance at 280 nm was collected, where this peak was determined to be the monomeric UBA(1) domain. The 5.6 kD, 0.5 ml fractions were collected, pooled, and concentrated using a 3,500 MWCO membrane to a concentration of 0.17 ug/ul (~31.2 uM UBA(1)). Pure bovine insulin isolated from the pancreas (Sigma-Aldrich) was used as a protein standard because its molecular weight and isoelectric point were similar to the UBA(1) domain (5.733 kD and 5.3, respectively). As mentioned, because of insulin's low solubility at pH 7, insulin was solubilized using a UBA pH 8 buffer (100 mM NaCl, 50 mM $NaH_2PO_4 \cdot H_2O$).

Native gel electrophoresis was performed using a Phast System, where a PhastGel that was premade was used. Briefly, 40 ml of Coomassie brilliant blue dye was mixed with 40 ml of 20% acetic acid and filtered. Eighty microliters of this dye was used to run the gel. The polyacrylamide gel was taken out of a 4 ˚C fridge, and 100 ul of MilliQ H_2O was applied onto the gel bed. The gel was subsequently placed on top of the watered gel bed inside the apparatus with the cover slip facing up. The cover slip was removed from the gel, and the gel was placed in the gel holder with buffer strips. The electrodes were lowered onto the buffer strips, and 1 ul

samples were loaded into wells with the gel being run at 200 V. The gel was stained for approximately 1 hr. and destained for 30 minutes.

2E: Matrix-Assisted Laser Desorption/Ionization Time of Flight (MALDI-ToF) mass spectrometry

After the monomeric HHR23A UBA domains were collected from FPLC size exclusion chromatography, the 0.5 ml fractions were collected, pooled, and concentrated in a 3,000 MWCO concentrator. The A_{280} of UBA(1) and UBA(2) C26A were checked on a Beckmann Coulter UV-Vis spectrophotometer, and then diluted to ~2 uM using MALDI matrix as a solvent. For 1 ml of MALDI matrix solution, 700 ul of H_2O, 300 ul of acetonitrile, 1 ul of trifluoroacetic acid, 10 mg sinapic acid were combined. The matrix was subsequently vortexed and the appropriate volumes were aliquoted into sterile 1.7 ml Eppendorf tubes. The calculated UBA domain volumes were then added to the matrix to make up 2 uM solutions of each HHR23A UBA domain. Typically, 1-2 ul of 100 uM protein solution in UBA pH 6.5 buffer was added to 100 ul of matrix for a final concentration of 2 uM.

One to two microliter aliquots of each UBA domain were placed on a MSP 96 well plate for MALDI-ToF mass spectrometry. Matrix-associated laser desorption/ionization protein standards were also prepared, using 5 ul of premixed MALDI-ToF mass spectrometry standard to 5 ul of MALDI matrix. Equal volumes of samples and standards were pipetted onto the MSP 96 well plate. Samples were allowed to air dry on the plate for 10 minutes before being measured with the Bruker microflex MALDI-ToF mass spectrometer.

Standards were first calibrated to close approximations (less than 0.5 ppm) of their mass to charge ratios. Four standards were calibrated with the following mass to charge ratios: insulin (~5.6 kD + H)$^+$, ubiquitin (~8.5 kD + H)$^+$, cytochrome *c* (~12 kD + H)$^+$, and myoglobin (~17 kD

$+ H)^+$. After calibrations were applied, sample wells were then individually selected and hit with a short laser pulse for ionization. Peaks were selected using Flex Analysis software and saved and exported as PDF files. Several replications of each UBA domain were acquired and typical examples are reported.

2F: QuikChange Mutagenesis of Ubiquitin-Associated Domains

Mutagenesis was performed using the pGEX-2T UBA(2) domain plasmid. A sequence alignment of the human DNA excision repair protein HHR23A UBA domains which encompassed a repertoire of UBA domain homologues including Rad23 UBA domain from baker's yeast, and other UBA domains from mouse was available in the literature (Thomas D. Mueller, 2002). From the protein primary sequence alignment, it seemed reasonable to mutate the HHR23A UBA(2) cysteine at position 26 to a serine amino acid because HHR23A UBA(1) contains a serine at this position. However, after successfully preparing this mutation using PCR-based mutagenesis, we discovered the HHR23A UBA(2) C26S domain does not express well, as we obtained very little protein in its final pure form.

From Pymol modeling we used valine as a replacement of the cysteine residue because it seemed that this side chain would fit well into the hydrophobic environment of Cys26. We designed primers for the valine mutation and successfully made this mutation and expressed the UBA(2) C26V variant; however, we obtained very little protein after final purification via FPLC-size exclusion chromatography. We recovered a small amount of this protein, which did not appear to be well-folded based on the CD spectrum.

We selected alanine to replace the cysteine at position 26 in the UBA(2) domain, and designed forward and reverse primers using Agilent technologies primer design program. After

receiving our primers, we made 1:50 dilutions using MilliQ H_2O and measured their A_{260} with a Beckmann Coulter UV-Vis spectrophotometer to determine primer concentration. Primer stock solutions at 125 ng/ul were then prepared. Fifty ng of template pGEX-2T UBA(2) plasmid was used for the PCR reaction. A QuickChange Lightning Mutagenesis kit was used to carry out the cysteine to alanine mutation.

After PCR, the samples were treated with 2 ul of DPN1 restriction enzyme to digest the DNA parent non-mutant double stranded DNA. A standard transformation was subsequently carried out using 45 ul of *Escherichia coli* XL-Gold cells. The transformation mixture was added to 1 ml of SOC broth and incubated at 37˚C for ~ 1.5 hours and then sterile technique was used to spread cells on L-Amp plates. Distinct colonies were selected and DNA was purified using a Wizard Plus SV Miniprep purification system (Promega). After DNA was purified, its A_{260} and A_{280} was measured using a UV-Vis spectrophotometer to determine DNA concentration. Dilutions at 100 ng/ul were then submitted with their respective PGEX-2T forward and reverse primers to the Murdock lab at the University of Montana for sequence confirmation.

The UBA(2) C26A sample sequence information was analyzed using the Expasy database to confirm the C26A mutation. This DNA was then transformed into BL21 (DE3) *E. Coli* cells and grown for 16 hours in L-broth. The standard UBA domain growth protocol was used to express this protein. We were able to grow and express this mutation with high yields and purity (Fig. 3.7).

2G: Far UV Circular Dichroism Spectroscopy

2Gi: Guanidine Hydrochloride Chemical Denaturation

Purified HHR23A domains were buffer exchanged by centrifuge ultrafiltration into circular dichroism (CD) buffer (20 mM Tris, 40 mM NaCl, pH 7.0, filtered) 12 times to ensure protein was entirely exchanged into the CD buffer. The refractive indexes of both 6 M GuHCl (in CD buffer, filtered) and CD buffer were measured. Four refractive index (RI) values were recorded for both CD buffer and 6 M GuHCl, and these data were used to determine the exact concentration of 6 M GuHCl with Eq. 2.1:

$$([\text{GuHCl}] = 57.147(\text{RI GuHCl} - \text{RI CD}) + 38.68(\text{RI GuHCl} - \text{RI CD})^2 - 91.6(\text{RI GuHCl} - \text{RI CD})^3). \quad (\mathbf{2.1})$$

With our 6 M GuHCl solution, the actual GuHCl concentration was generally near 5.5 M. A 3 ml, 5 uM stock solution was prepared for each purified variant (UBA(1) and UBA(2) C26A), and an ~10 ml stock of 5 uM guanidine hydrochloride denatured UBA domain protein was made for each variant. The concentrations of the 5 uM native UBA peptides were checked using a Beckmann Coulter UV-Vis spectrophotometer.

The guanidine hydrochloride titration experiments were performed using an Applied Photophysics Chirascan CD spectrophotometer. Briefly, the instrument was initially purged with nitrogen gas to permeate the system, and subsequently the auto-titrator, lamp, and instrument were turned on and allowed to warm up for ~1 hour. A CD buffer blank was taken, auto-subtracted, and the guanidine hydrochloride melts were carried out by placing ~870 ul of 5 uM native protein in a clean 4 mm path length quartz cell with a stir bar. Two programmed syringes, one displacing 5 uM native protein from the cell, and the other inputting denatured 5 uM protein

into the cell, were used for the auto-titration experiment. These experiments were carried out at 298.15 K. Data were recorded from 0 – 5 M guanidine hydrochloride concentration, in steps of 0.1 M. One experiment took approximately 4.5 hours, and three replicates were done for each UBA variant. The guanidine melt data for these UBA variants were fit to a two state model, where a linear dependence of Gibbs free energy on guanidine hydrochloride concentration (Eq. 2.2) was used to determine the free energy of unfolding of these proteins in the absence of denaturant:

$$(\Delta G = -RT\ln K = \Delta G_0 - m[GuHCl]), \quad (\mathbf{2.2})$$

where ΔG and ΔG_0 are the free energy of unfolding in the presence and absence of GuHCl, and m is the dependence of ΔG on GuHCl concentration (Yoshihisa Hagihara, 1993).

2Gii: Thermal Denaturation

Thermal denaturation experiments for all UBA(1) domain concentrations were done with purified protein in UBA pH 6.5 buffer (presumed monomeric UBA(1) domain protein collected from FPLC). Concentrations of 2.5 uM, 5 uM, 20 uM, 50 uM, and 100 uM UBA(1) protein at 3 ml volumes were prepared from concentrated stocks of UBA(1), and their A_{280} was measured using a Beckmann Coulter UV-Vis spectrophotometer subtracting the UBA pH 6.5 buffer blank or the sample's A_{350} from its A_{280}, whichever value was greater, to get an accurate determination of the protein concentration. The following path length quartz cells were used for the following UBA(1) concentrations: 2.5 uM (1 cm), 5 uM (1 cm), 20 uM (4 mm), 50 uM (4 mm), and 100 (1 mm). After concentration was confirmed, the Applied Photophysics Chirascan CD spectrophotometer was turned on following the same protocol mentioned in the guanidine hydrochloride melt methodology. A temperature controller was turned on and a thermocouple

was placed in each sample cell along with a stir bar to monitor temperature changes for these experiments. A UBA pH 6.5 buffer blank was taken from 250 to 200 nm, and these data were auto-subtracted to obtain a baseline near zero. Thermal melt experiments were carried out by first taking a secondary structure scan from 250 to 200 nm to confirm α-helix, and then wavelength was adjusted to 222 nm to monitor melting of this α-helical trough. The temperature was initiated at 6 ˚C, and the temperature was increase at a rate of 2 ˚C per minute. Data at 222 nm were recorded in 2˚C intervals until the temperature reached approximately 90 ˚C.

After the temperature ramping experiments at 222 nm, the temperature was lowered back to initial starting temperature, and a 250-200 nm scan was taken to determine whether native secondary structure was restored. The temperature melt data were analyzed using SigmaPlot and fitting the temperature denaturation data using the following:

$$\frac{dlnK}{d(\frac{1}{T})} = -\frac{\Delta H}{R} \qquad \textbf{(2.3)}$$

$$(\Delta G_u = -RTln(K_u) = \Delta H_m\left(1 - \frac{T}{Tm}\right) - \Delta C_p[(T - T_m) + Tln\left(\frac{T}{Tm}\right)] \qquad \textbf{(2.4)}$$

These equations were used to examine the Gibbs free energy of unfolding as a function of temperature. For ΔC_p, the value of 0.45 kcal/mol was used from a HHR23A UBA(2) domain thermodynamic study (Ginka S. Buchner, 2012). The Van't Hoff (2.3) enthalpies and melting temperature values agreed well with the Gibbs-Helmholtz fits, thus we only fit our thermal melt data to the Gibbs-Helmholtz thermodynamic equation (2.4).

Chapter 3: Results

3A: Introduction

Juli Feigon and colleagues determined that the HHR23A UBA(1) domain does not appear to show evidence of dimerization into the 3 mM concentration range using NMR spectroscopy line-width broadening (Thomas D. Mueller, 2002). Moreover, while these isolated HHR23A UBA domains do not appear to interact with their own UBA domains, the question was addressed whether or not the HHR23A UBA(1) and UBA(2) domains interact with each other. As Mueller et. al. mentioned, if HHR23A UBA(1) and UBA(2) domains interacted together, then dimerization would not be observed for these individual HHR23A UBA domains. The yeast RAD23 homologue of human HHR23A was discovered to homodimerize, so the question needed to be answered whether HHR23A UBA(1) and UBA(2) domains interact. To address this question, we mixed these domains in equimolar amounts and subjected these samples to FPLC size exclusion chromatography.

After our final purification of the HHR23A UBA(1) domain, our MALDI-ToF mass spectrum suggested potential dimerization (Fig. 3.1). Because Feigon et. al examined dimerization of the HHR23A UBA(1) domain in the mM concentration range via NMR line width broadening, it was a relevant question to determine whether the HHR23A UBA(1) and UBA(2) domains are forming quaternary structures in the uM concentration range. When we searched the literature, we discovered that the human ubiquitin scaffold protein p62 does homodimerize in the uM concentration range, and plays an important functional role with ubiquitin signaling (Jed Long, 2010). We tested these questions of HHR23A UBA domain dimerization using FPLC size exclusion chromatography and far UV CD spectroscopy thermal denaturation.

It is important to know whether HHR23A UBA domains form quaternary structure, so we carried out a careful re-evaluation of dimerization of UBA(1), UBA(2), cross-reaction of UBA(1) and UBA(2), and the interaction of these UBA domains with ubiquitin.

3B: Ubiquitin-Associated Domain MALDI-ToF Observations

After the HHR23A UBA domains were purified, the MALDI-ToF mass spectra showed two distinct peaks in both mass spectrograms (Figs. 3.1, 3.2). In Fig 3.1, a peak at m/z = 5,634.951 corresponds to molecular weight (MW) of UBA(1) monomer (5,635.3 g/mol), while in Figure 3.2, a peak of m/z = 5,258.922 corresponds to MW of UBA(2) C26A monomer (5,259.81 g/mol). In Figure 3.1 a peak at m/z = 11,269.220 corresponds to MW of UBA(1) dimer (11,270.6 g/mol), while in Figure 3.2 a peak at m/z = 10,521.609 corresponds to MW of UBA(2) C26A dimer (10,519.62 g/mol).

Interestingly, these observations suggested the possibility of micromolar dimerization as was discovered in the p62 UBA domain. Therefore, we carried out a set of experiments to ascertain whether dimerization occurs or alternatively, if the MALDI matrix environment induces these domains to form quaternary structure. We assayed dimer formation by FPLC size exclusion chromatography: HHR23A UBA(1) dimerization dependence on concentration, cross reaction of UBA(1) with UBA(2), and interaction of these HHR23A UBA domains with ubiquitin.

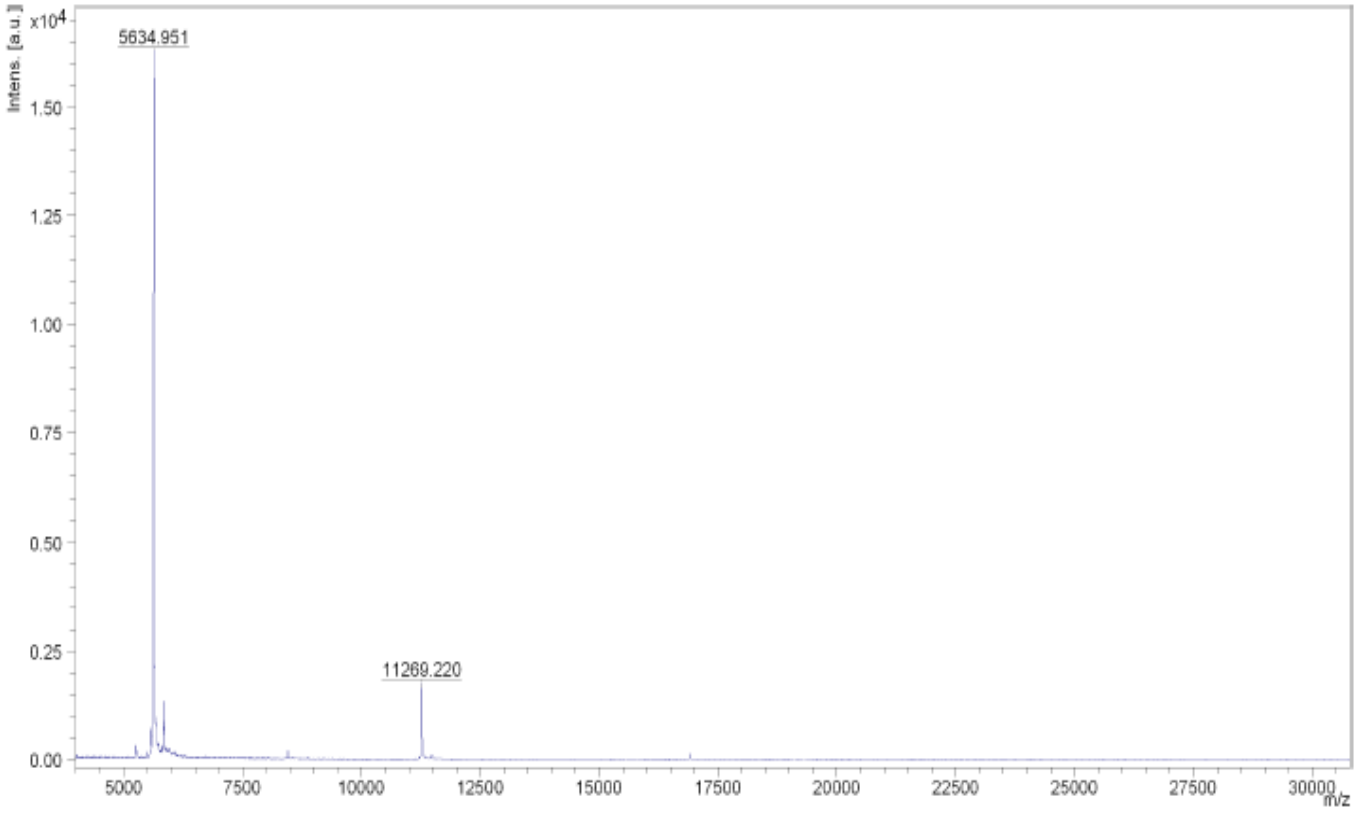

Fig. 3.1. HHR23A UBA(1) domain depicting the monomeric peak at 5,634 m/z and the less intense dimeric peak at 11,269 m/z standardized with insulin (~5,600 m/z), ubiquitin (~8,500 m/z), cytochrome *c* (~12,000 m/z), and myoglobin (~17,000 m/z). Sample was run in at least two separate protein preparations all revealing the same mass spectrum.

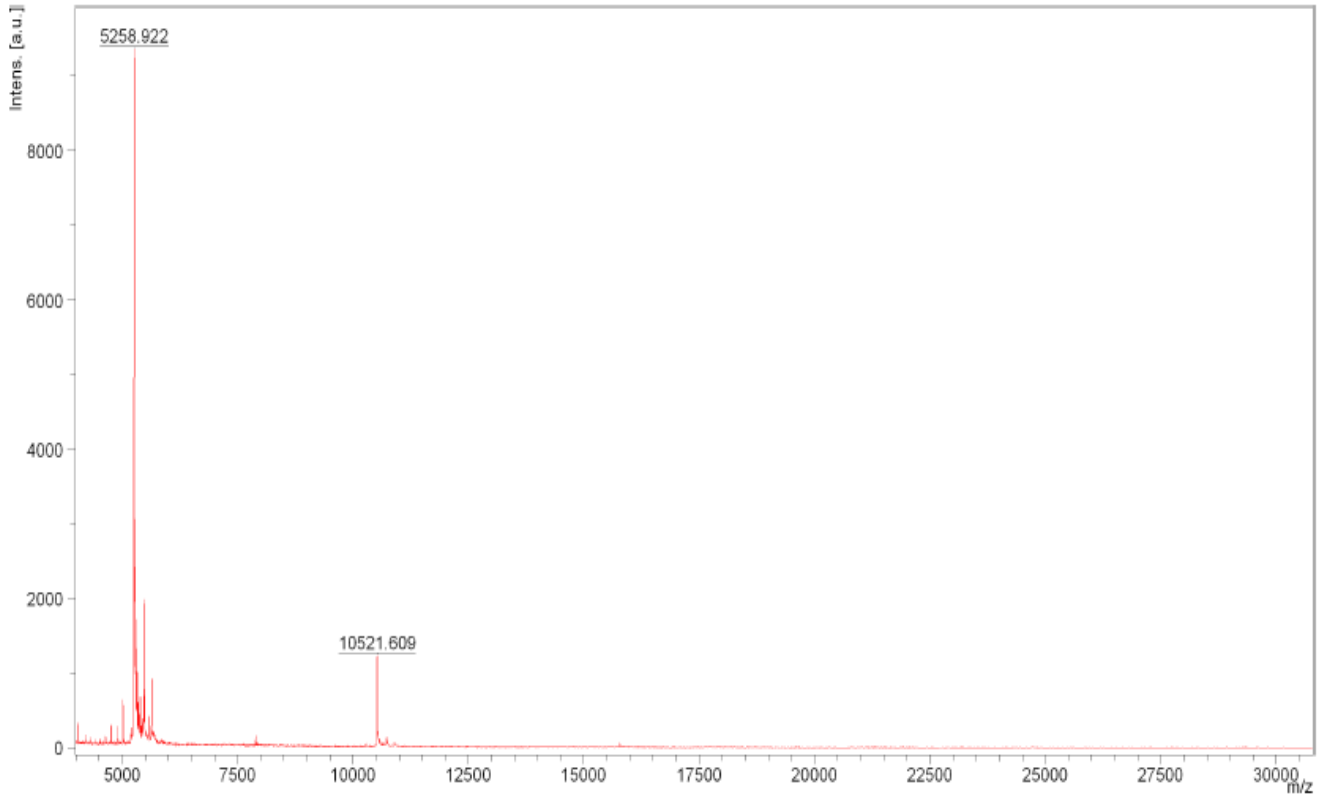

Fig. 3.2. HHR23A UBA(2) C26A domain depicting the monomeric peak at 5,258 m/z and the less intense dimeric peak at 10,521 m/z standardized with insulin (~5,600 m/z), ubiquitin (~8,500 m/z), cytochrome *c* (~12,000 m/z), and myoglobin (~17,000 m/z). Sample was run in at least two separate protein preparations all revealing the same mass spectrum.

3C: Size-Exclusion Chromatography of Ubiquitin-Associated Domains

A question that needed to be answered was whether dimerization of HHR23A UBA domains occurs in the micromolar concentration range. Our MALDI-ToF data show that both UBA(1) and UBA(2) C26A domains dimerize at ~2 uM concentration. FPLC size-exclusion chromatography (SEC) data show that HHR23A UBA domains elute from Superdex 300/10 GL column at ~12 ml, and equine cytochrome *c* elutes at ~ 10 ml (Fig. 3.3). This experiment was replicated twice. Different concentrations of the equine cytochrome *c* standard (600 and 300 uM) elute from the column at similar volumes (data not shown), suggesting that even as the concentration of the horse heart cytochrome *c* is varied, this protein elutes as a monomer.

Because cytochrome *c* (MW = ~12 kD) eluted from the Superdex 300/10 GL column at ~10 ml, and our UBA domains eluted later, we confirmed that the HHR23A UBA domains elute as monomers. As a followup experiment, an SDS-PAGE of these elution fractions was performed to confirm our observations of our FPLC-SEC data (shown in section 3D).

It was next a question of determining a change in the elution volume of HHR23A UBA(1) domain. We examined this question of UBA(1) domain dimerization by keeping FPLC-SEC conditions fixed but varying UBA(1) concentrations. Proteins chromatographed at concentrations of 600, 100, and 50 uM show similar elution volumes (Fig. 3.4). We did encounter signal issues when concentrations were tried below UBA(1) 50 uM. Moreover, the 600, 100, and 50 uM UBA(1) curves overlap nicely, but it appears that the 600 uM UBA(1) concentration seems to be converted more towards a dimer molecular weight of 11.2 kD (Fig. 3.4). The loading conditions for these samples are not identical, which may influence the elution volume changes observed for these different UBA(1) domain concentrations.

To ascertain whether the HHR23A UBA(1) or UBA(2) C26A domains interact with bovine ubiquitin, we prepared 100 uM of both UBA domains and ubiquitin, and then mixed them in equimolar amounts with a varied incubation time to determine any interaction. Initially, these experiments were carried out with a 5 minute incubation time; however, we discovered that a longer incubation time of approximately 15 minutes was needed to observe interaction of UBA(1) with ubiquitin, as an earlier elution volume than the 10 ml elution volume of cytochrome *c* was observed (Fig. 3.5). There appeared to be no interaction of UBA(2) C26A with ubiquitin, although we had signal to noise issues with our runs, and so this experiment needs to be repeated (data not shown) before coming to a firm conclusion.

Juli Feigon and colleagues asked whether these HHR23A UBA domains interact with each other. If homodimerization is not observed for the UBA(1) and UBA(2) domains, then could both the UBA(1) and UBA(2) domains interact together? To test this question qualitatively, we used equimolar amounts of 100 uM UBA(1) and 100 uM UBA(2) C26A and discovered that these UBA domains do not interact with each other (incubation times of 10 min, 25 min, and 14 hours) at these equimolar concentrations, and the incubations times observed seem to be unimportant, as all curves overlay on top of each other (10 min, 25 min, and 14 hours, Fig. 3.6). In addition, pure bovine ubiquitin and UBA(1) standards were used to detect this interaction, and the UBA(1) monomer overlays nicely with these data (Fig. 3.6).

To determine homodimerization of the HHR23A UBA(1) domain quantitatively, we subjected this protein to concentration dependent thermal unfolding experiments.

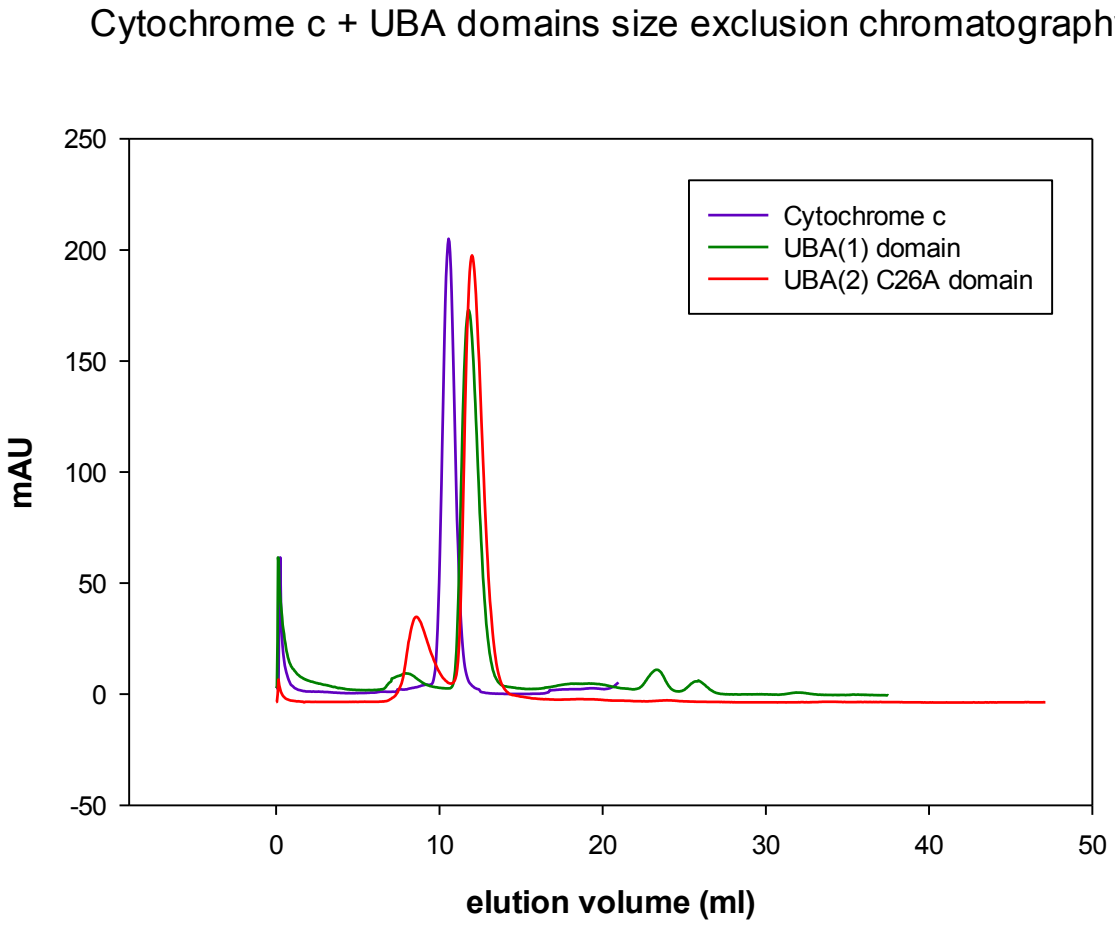

Fig. 3.3. Overlay of the HHR23A UBA(1) and UBA(2) C26A domains at 100 uM concentrations eluting as monomer. 300 uM, 12 kD cytochrome *c* shown as a standard.

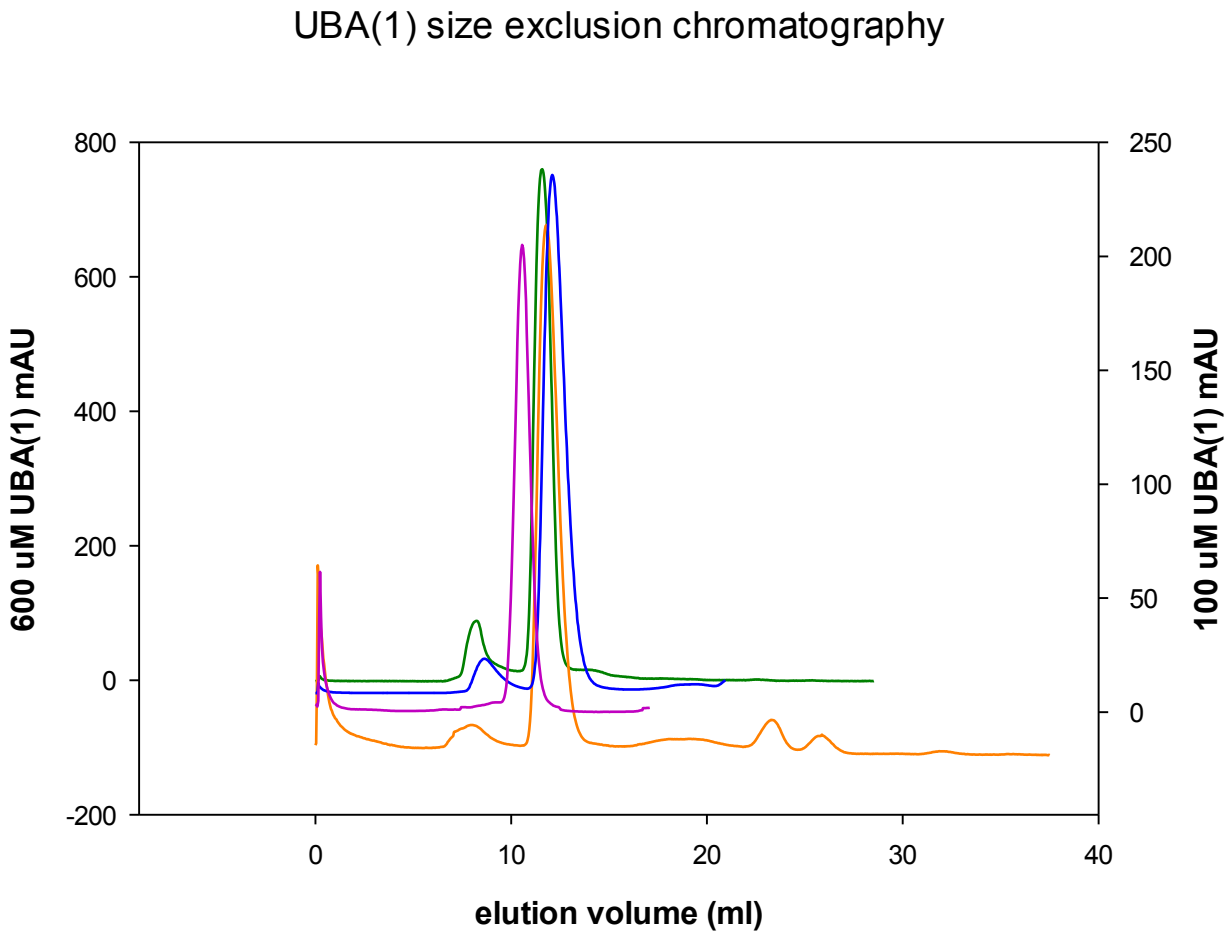

Fig. 3.4. Concentration variation of the UBA(1) domain to assess elution shift. 600 uM UBA(1) (green), 300 uM UBA(1) (orange), 100 uM UBA(1) (blue) all show monomeric elution volumes using a 600 uM, 12 kD cytochrome *c* standard (purple).

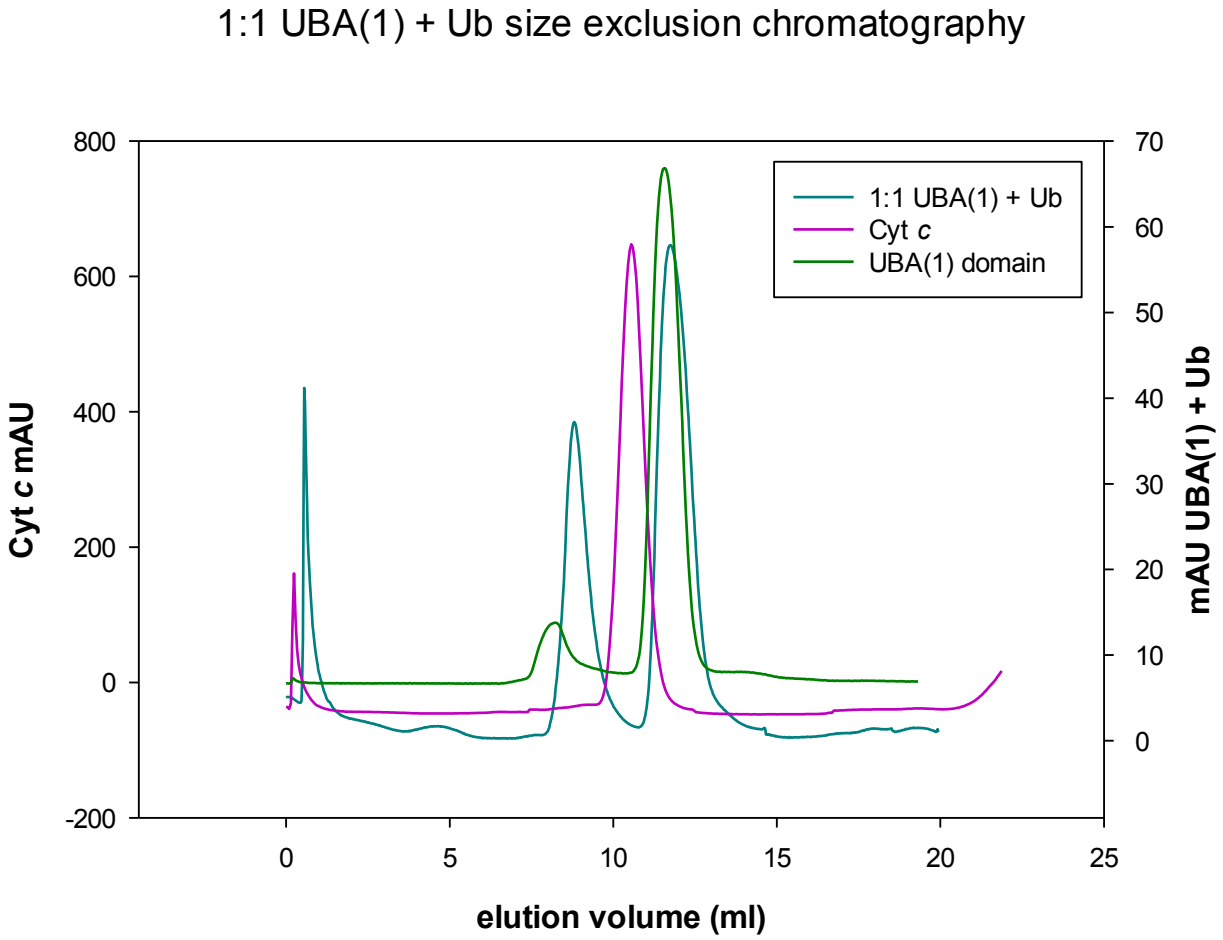

Fig. 3.5. FPLC SEC data depicting interaction of ubiquitin (Ub) with UBA(1) domain at 25 minutes incubation in pH 6.5 buffer. Interaction does occur between UBA(1) and bovine ubiquitin.

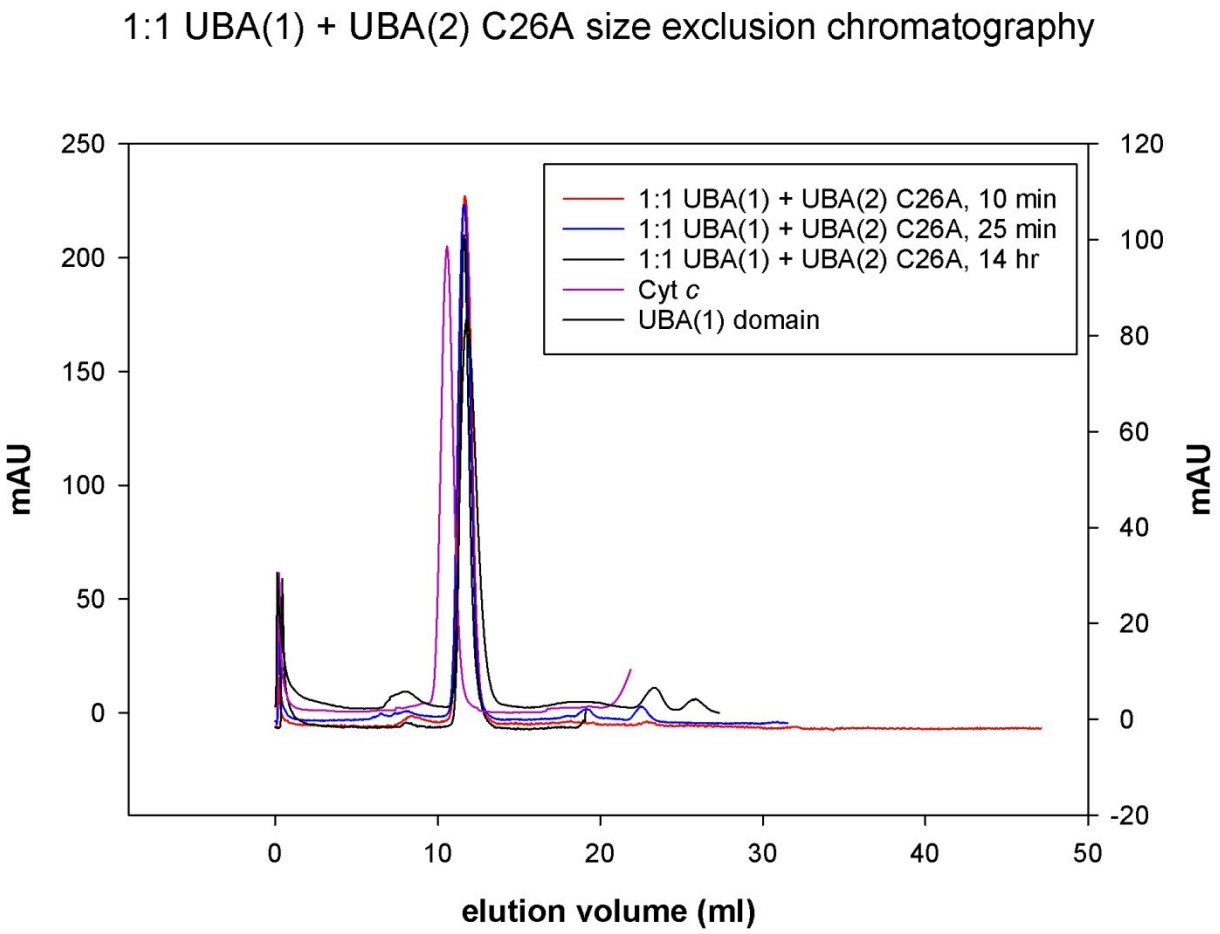

Fig. 3.6. FPLC size-exclusion chromatography showing equimolar concentrations (50 uM) of UBA(1) and UBA(2) C26A mixed together in UBA pH 6.5 buffer at different incubation periods. Cytochrome *c* and UBA(1) domains are shown as standards.

3D: SDS-PAGE of FPLC-SEC Fractions

From the size exclusion chromatography data, it became a goal to characterize these early eluting fractions in each of the FPLC-size exclusion chromatograms (Fig. 3.3). These lower elution volumes with small absorbance eluted off the column before the ~12 kD cytochrome *c*, implying that these eluents had larger molecular weight than 12 kD. However, the literature suggested that some UBA domains are in monomer-dimer equilibrium, and in this way, it was unclear whether this lower elution volume peak could be higher order oligomers of these UBA domains (Shin Isogai, 2011). To ascertain these early eluting peaks, the FPLC-SEC 0.5 ml fractions containing these eluents were collected and pooled into clean, separate 3,000 MWCO concentrators. These fractions were subsequently concentrated at 4 ˚C, 3,500 rpm for 15 minute cycles until their solution volumes were approximately 500 microliters. The A_{280} from these samples were measured, and the assumption was made that these early eluting peaks were residual Glutathione S-transferase (from the biotinylated thrombin cleavage reactions). Therefore, their A_{280} was calculated as if these early elution volumes were Glutathione S-transferase and not UBA domains (see Methods 2A).

In addition, the following samples were run as standards or controls for determination of the early elution unknown volumes from UBA(1) and UBA(2) C26A size exclusion chromatograms: pure UBA(1), pure UBA(2) C26A, cut GST, GST-UBA(1) fusion protein, Bio-Rad precision plus protein standard, as well as UBA(1) and UBA(2) C26A post GST thrombin cleavage but before final purification.

A problem with identifying these early elution volumes was that the UBA(1) domain lower elution volume peak was difficult to concentrate to obtain enough protein to show up on the SDS-PAGE. This is evident by comparing the UBA(1) domain prior to size exclusion

chromatography and post size exclusion purification from the gel, where there is a residual amount of the this lower elution eluent (Fig. 3.7). Although the early eluting unknown peak from the UBA(1) domain size exclusion chromatography was not detected, the overlay of UBA(1) domain and UBA(2) C26A domain chromatograms demonstrate that this early eluting unknown peak is of similar molecular weight (Fig. 3.3).

Moreover, the early elution volume from the UBA(2) C26A chromatography was identified via SDS-PAGE, and was determined using the Bio-Rad precision plus protein standard to be Glutathione S-transferase, which has an approximate molecular weight of ~26 kD. Therefore, the lower elution volumes with minimal absorbance that were thought to be potentially UBA domain quaternary structure turn out to be residual Glutathione S-transferase. However, this did not rule out the possibility that these HHR23A domains could be forming quaternary structure, so we subjected the HHR23A UBA(1) to native polyacrylamide gel electrophoresis, using a 30 uM concentration that would monitor this UBA(1) dimerization in the uM concentration range.

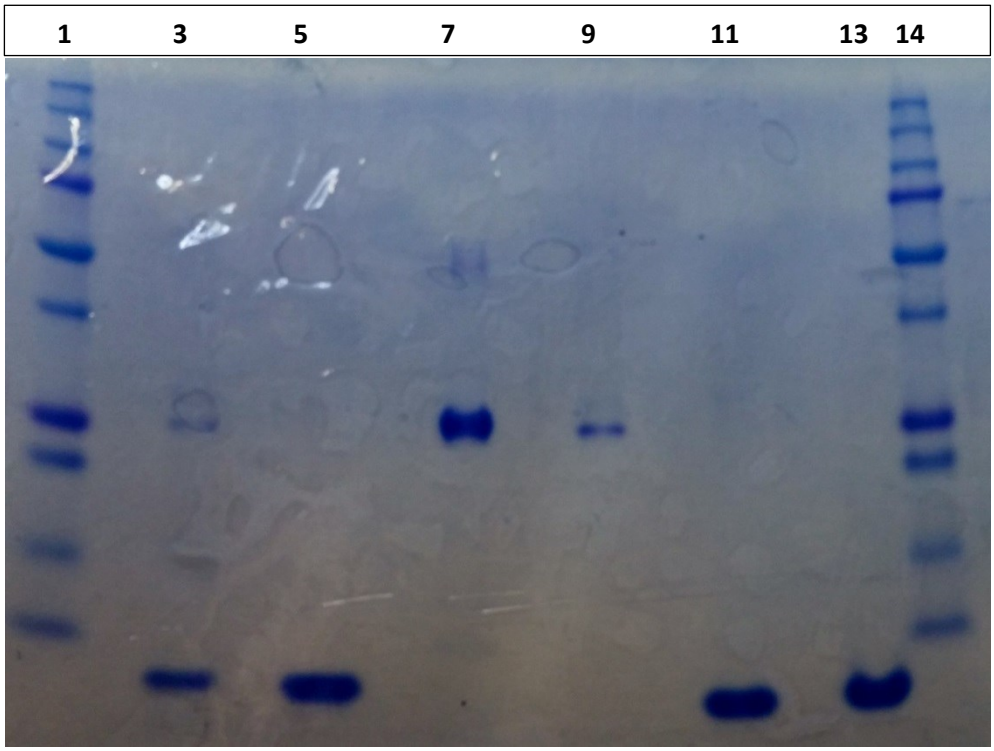

Fig. 3.7. SDS-PAGE depicting the UBA(1) and UBA(2) C26A domains with lanes 1 and 14 representing Bio-Rad precision plus standards. The following lanes depict these samples: UBA(2) C26A before SEC (lane 3), UBA(2) C26A after SEC (lane 5), UBA(1)-GST (lane 7), low elution volume UBA(2) C26A peak (lane 9), UBA(1) before SEC (lane 11), UBA(1) after SEC (lane 13).

3E: Native-PAGE of Ubiquitin-Associated Domain 1

It had been shown that a monomer-dimer equilibrium does occur with the mouse p62 UBA domain (Shin Isogai, 2011). Additionally, we were curious if dimerization occurs in the absence of sodium dodecyl sulfate. In this way, we subjected the HHR23A UBA(1) domain to native polyacrylamide gel electrophoresis to determine whether or not we observe dimer or monomer. Figure 3.8 lanes two and four show that our UBA(1) domain migrates down the gel as a monomer with the same mobility as insulin (pI of UBA(1) is 5.1, pI of insulin is 5.3). We used pure insulin from bovine pancreas (Sigma-Aldrich) as a standard, and UBA(1)-GST and pure bovine ubiquitin from erythrocytes (Sigma-Aldrich) as additional markers. We had issues with potential aggregation with ubiquitin (Fig. 3.8). The concentration of ubiquitin was calculated to be ~200 uM using MilliQ H_2O as a solvent (based on recommendations from Sigma-Aldrich), so it is possible that ubiquitin may be forming higher order oligomers under these concentration conditions. In addition, there were concentration issues with insulin, as this protein comes in a lyophilized powder and was difficult to equate to the HHR23A UBA(1) domain concentration of 30 uM. Next we analyzed HHR23A UBA domain thermodynamics using far UV CD guanidine hydrochloride titration.

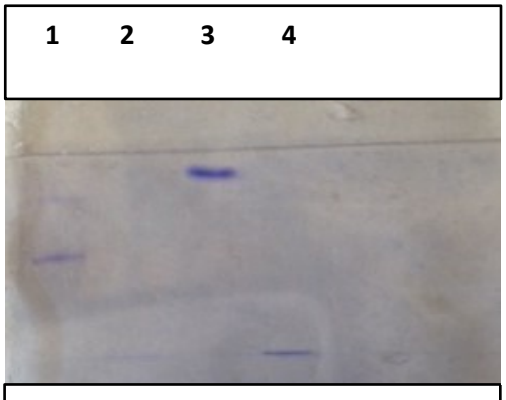

Fig. 3.8. Native-PAGE of HHR23A UBA(1) domain. Lane 4 is monomer at 31 uM. Lane 1 = UBA(1)-GST, lane 2 = insulin, lane 3 = ubiquitin

3F: Thermodynamics of Ubiquitin-Associated Domains

3Fi: Guanidine Hydrochloride Denaturation

Our guanidine hydrochloride titration data demonstrate that the Gibbs free energy of unfolding for the HHR23A UBA(1) domain is 2.97 ± 0.05 kcal/mol. For comparison, Burcu Anil et. al. carried out a guanidine hydrochloride melt of the HHR23A UBA(2) domain and calculated the Gibbs free energy of unfolding to be 1.34 ± 0.06 kcal/mol (Burcu Anil, Benben Song, Yuefeng Tang, Daniel P. Raleigh;, 2004). Furthermore, our HHR23A UBA(2) C26A increased the stability (Table 3.1) of this HHR23A C-terminus domain, suggesting that this C26A mutation located between helices 2 and 3 of the UBA(2) domain stabilizes the structure. The cysteine at position 26 is flanked by a hydrophobic environment (Fig. 1.1.), where cysteine may be a part of the hydrophobic core of HHR23A UBA(2) domain. The cysteine residue does not appear to be near the surface of this protein (Thomas D. Mueller, 2002). Juli Feigon et. al. also demonstrate a potential hydrophobic surface for both HHR23A domains, which are considered to be binding sites for protein-protein interaction (i.e. ubiquitin). The cysteine at position 26; however, is not located on the surface (Thomas D. Mueller, 2002).

The cooperativity of unfolding in these HHR23A domains are similar (m-values, Table 3.1), indicating that their transitions from folded to unfolded are similar under denaturing conditions and that they share common buried hydrophobic surface area (Myers JK, 1995). Because of their similar m-values, indicative of similar changes in heat capacities, we performed a thermal denaturation to determine the changes in the equilibrium of unfolding K_u by varying UBA(1) domain concentrations.

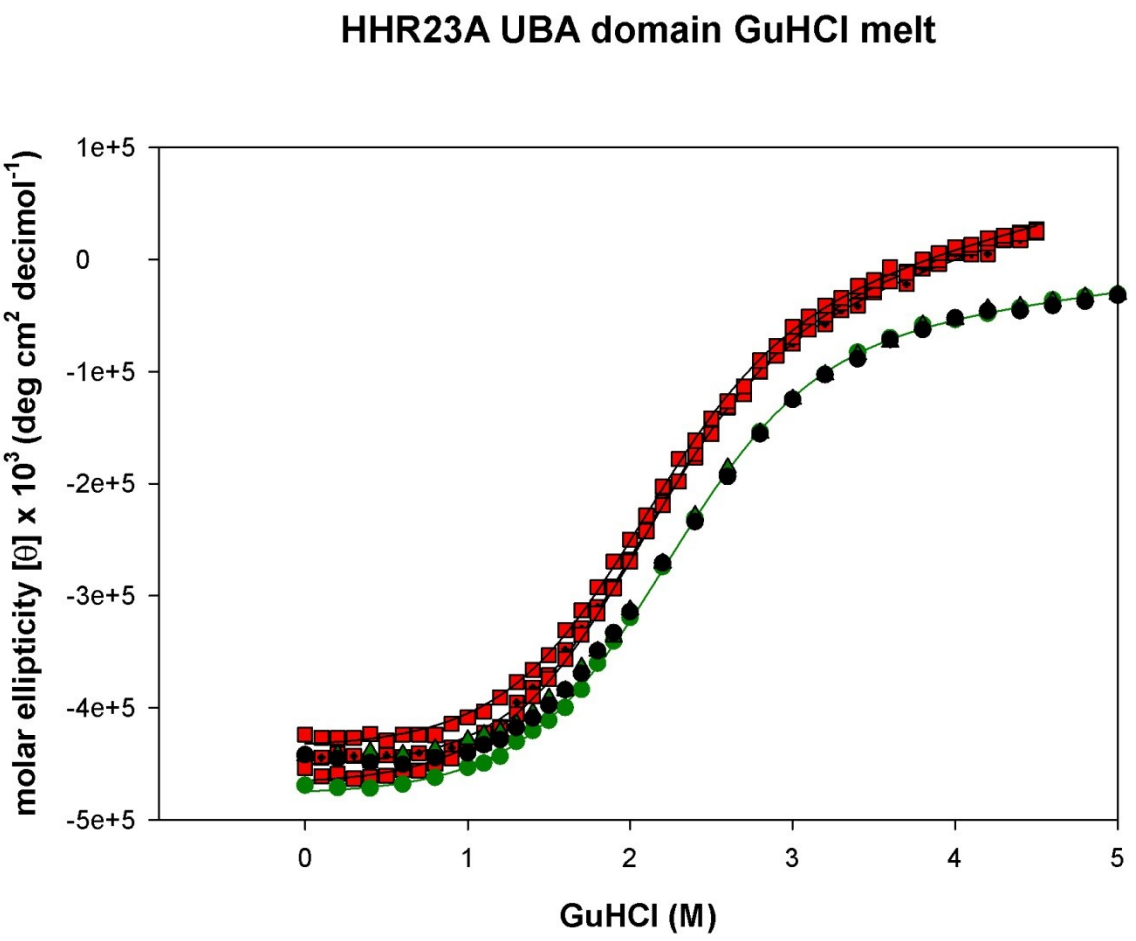

Fig. 3.9. Chemical denaturation of the HHR23A internal domain (UBA(1), green, black) and C-terminal domain with a C26A mutation (UBA(2), red). UBA(1) domain shows greater stability of UBA(2)

HHR23A UBA domain	ΔG_u (kcal/mol)	m (kcal/mol)	C_m (M)
UBA(1)	**2.97 ± 0.05**	**1.34 ± 0.01**	**2.22 ± 0.02**
UBA(2)	**1.34 ± 0.06**	**1.12 ± 0.01**	**1.19 ± 0.01**
UBA(2) C26A	**2.66 ± 0.06**	**1.28 ± 0.04**	**2.06 ± 0.04**

Table 3.1. Thermodynamic parameters depicting the free energy of unfolding for the HHR23A internal domain (UBA(1)) and the C-terminal domain (UBA(2) C26A). The C26A mutation in the UBA(2) domain increases the stability of UBA(2) (Burcu Anil, Benben Song, Yuefeng Tang, Daniel P. Raleigh;, 2004).

3Fii: Thermal Denaturation of UBA(1) Domain

To quantitatively evaluate potential homodimerization of the HHR23A UBA(1) domain, we subjected this internal domain to a series of heat denaturation experiments by varying protein concentrations and using far UV circular dichroism spectroscopy to monitor secondary structure. If the protein dimerizes we expect an increase in the melting temperature in the concentration range where dimerization is hypothesized to occur (Jed Long, 2010). We discovered that as the protein is scanned in the far UV region before and after temperature ramping of the protein, that the spectra overlay quite nicely indicating renaturation of this compact three helix bundle and hence implying reversible processes (Fig 3.10-3.13). In this way, the data are suitable for extracting thermodynamic parameters using the Gibbs-Helmholtz thermodynamic equation (Eq. 2.4, Materials & Methodology). All concentrations of HHR23A UBA(1) domain were normalized independent of protein concentration, and their secondary structures overlapped nicely before and after the temperature unfolding at 222 nm (Fig 3.14).

In addition, the thermal denaturation experiments were carried out as a function of UBA(1) domain concentration (Figs. 3.15-3.18). Their melting curves were overlaid and they demonstrate a reasonable fit with each other qualitatively, visually indicating no change in the melting temperature and thus no change in the equilibrium constant K_u (Fig 3.19). To assess a change in the enthalpy of unfolding and a transition in the melting temperature, the thermodynamic parameters were calculated for the UBA(1) domain at each protein concentration (Table 3.2). No significant change in the thermodynamic parameters, T_m and ΔH_m, are observed as concentration increases, indicating no UBA(1) quaternary structure in the micromolar concentration range. A graph of melting temperature, T_m, versus UBA(1) domain concentration is shown in Figure 3.20, showing the mean T_m values and low standard deviations. The 5 uM

concentration had a larger standard deviation than higher UBA(1) domain concentrations, so a 2.5 uM concentration heat denaturation experiment was performed and showed consistency in the melting temperature and unfolding enthalpy (Table 3.2).

In this way, we are not observing dimerization of the HHR23A UBA(1) domain in the micromolar concentration range, which is different from what is observed with the p62 UBA domain. These differences in quaternary structure in low concentration ranges may relate to the functions of these proteins: p62 is an ubiquitin scaffolding protein and HHR23A is a nucleotide excision repair protein.

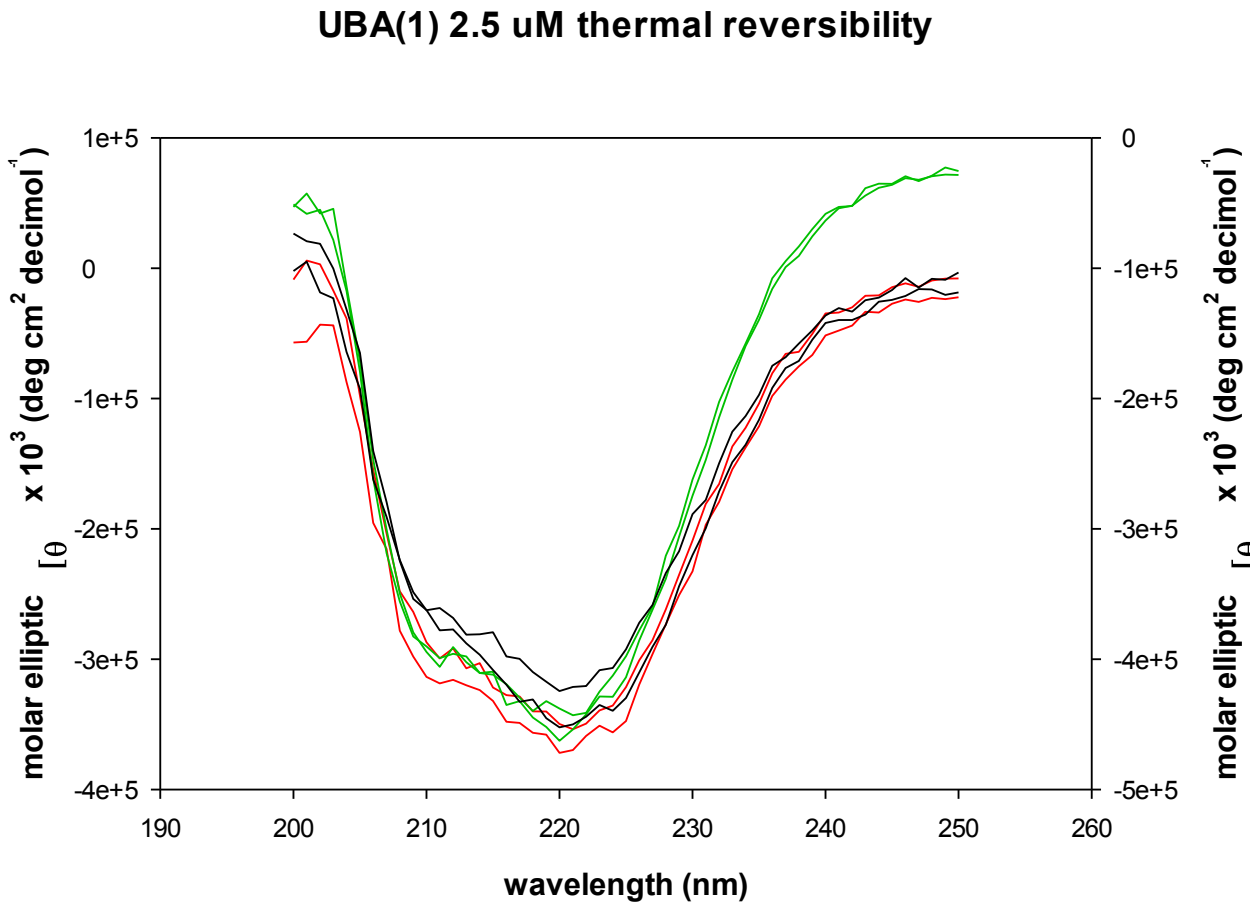

Fig. 3.10. Overlay of three replications (green, red, and black) at 2.5 uM UBA(1) domain concentration showing initial and final scans for the temperature melts, indicating renaturing to α-helix secondary structure and thus reversible processes.

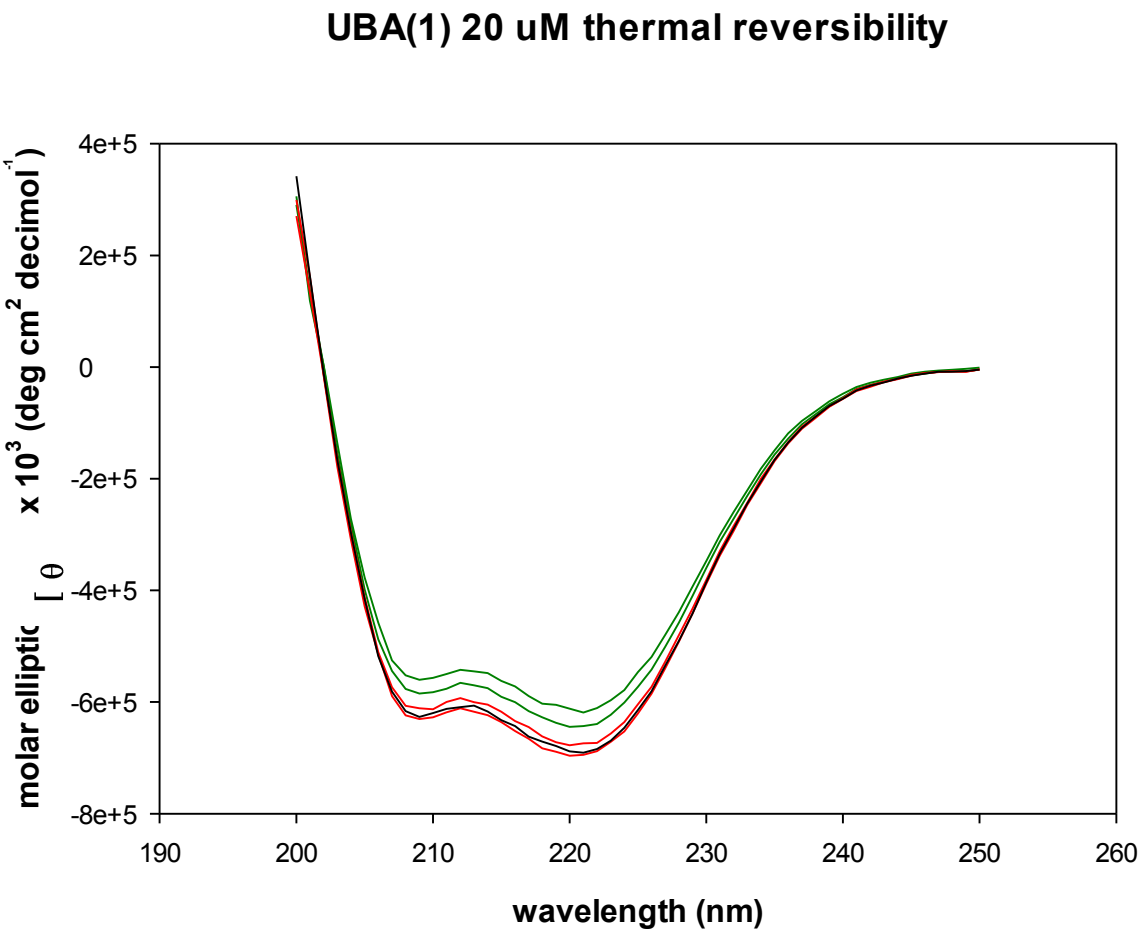

Fig. 3.11. Overlay of three replications (green, red, and black) at 20 uM UBA(1) domain concentration showing initial and final scans for the temperature melts, indicating renaturing to α-helix secondary structure and thus reversible processes.

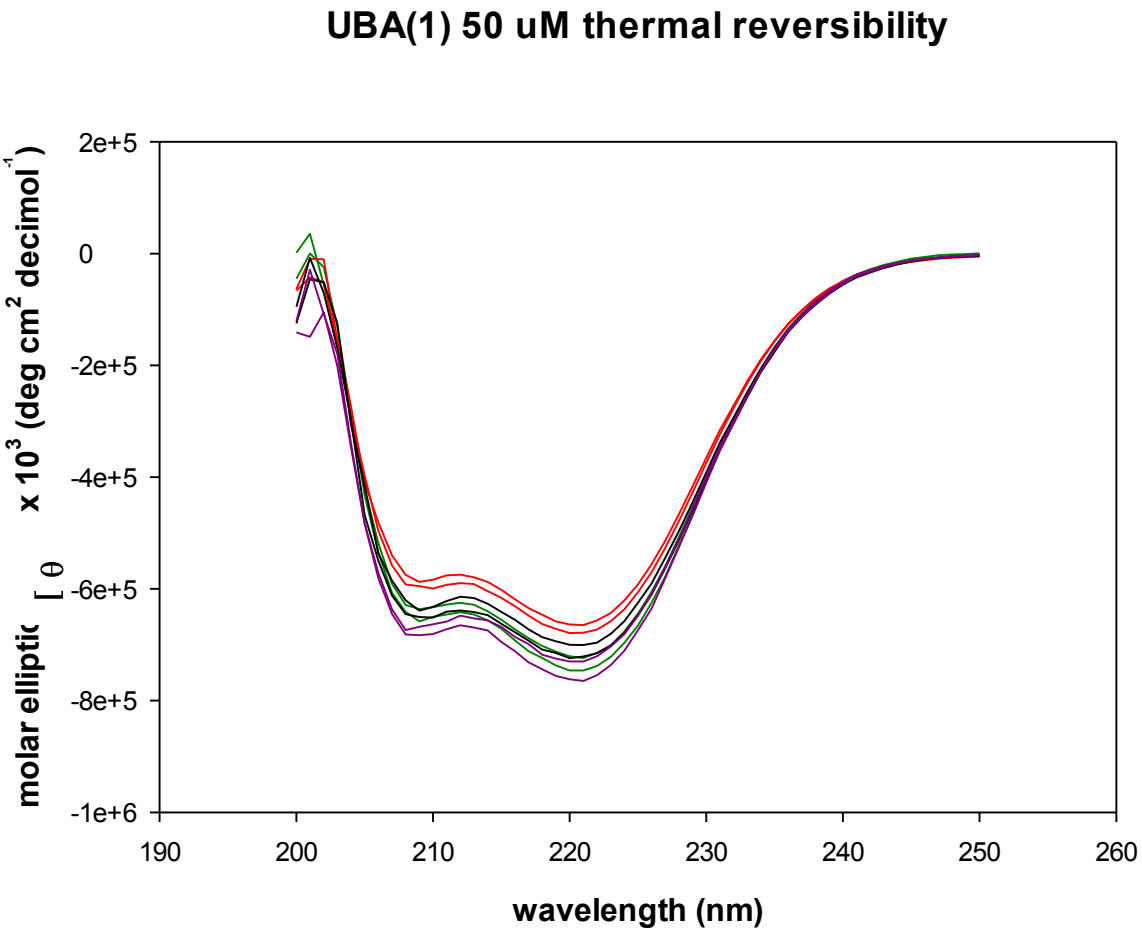

Fig. 3.12. Overlay of four replications (green, red, black, and purple) at 50 uM UBA(1) domain concentration showing initial and final scans for the temperature melts, indicating renaturing to α-helix secondary structure and thus reversible processes.

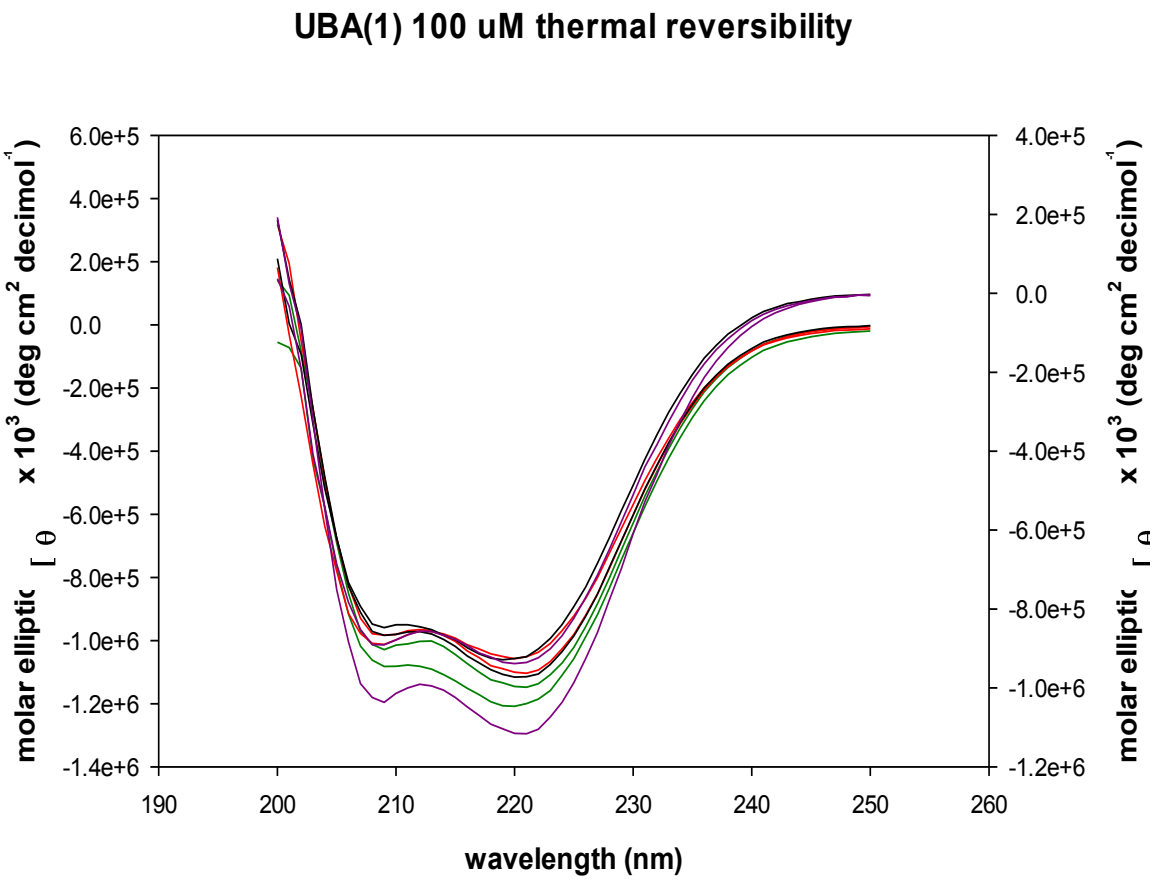

Fig. 3.13. Overlay of four replications (green, red, black, and purple) at 100 uM UBA(1) domain concentration showing initial and final scans for the temperature melts, indicating renaturing to α-helix secondary structure and thus reversible processes.

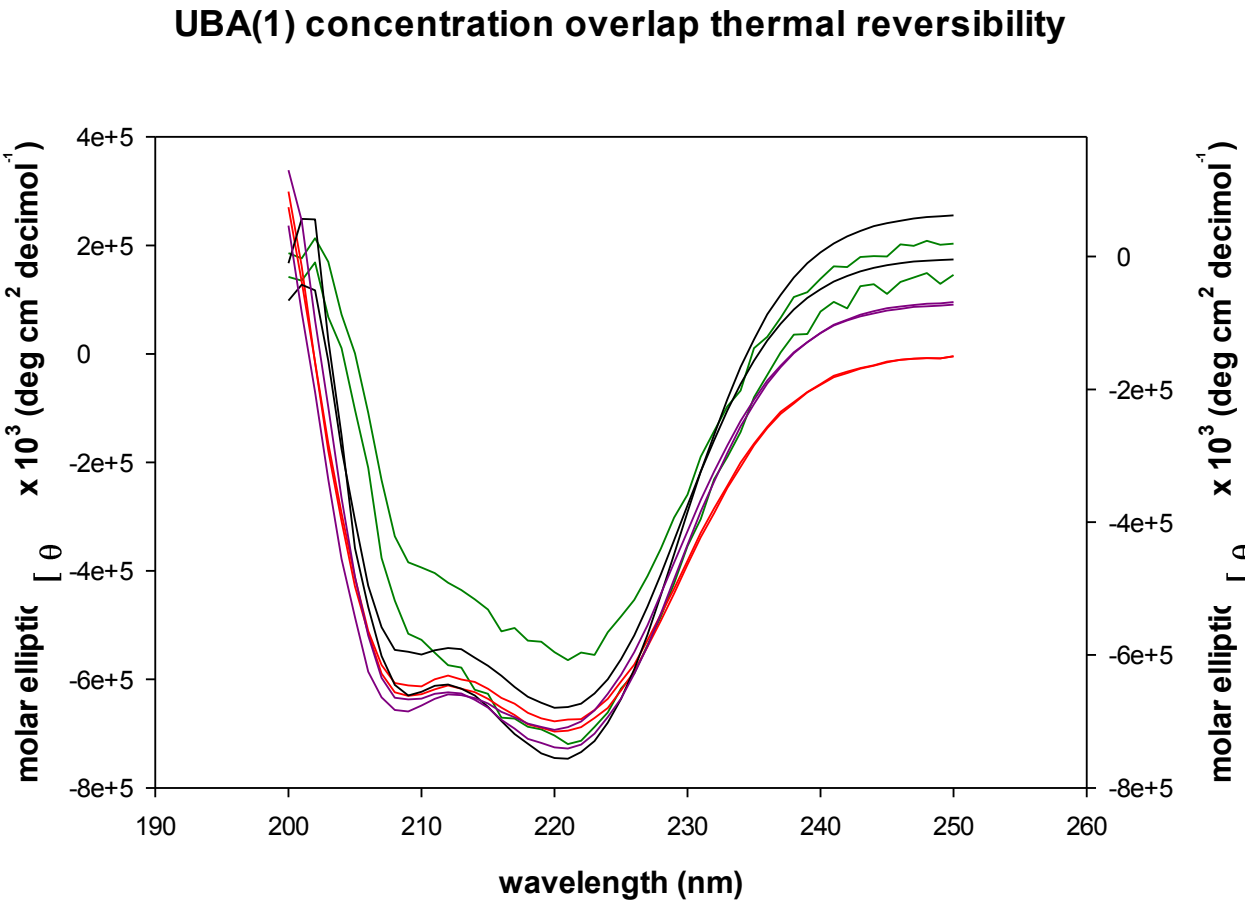

Fig. 3.14. Overlay of 5 uM (green), 20 uM (red), 50 uM (black), and 100 uM (purple) initial and final scans for the temperature melts showing renaturing to α-helix secondary structure and thus reversible processes.

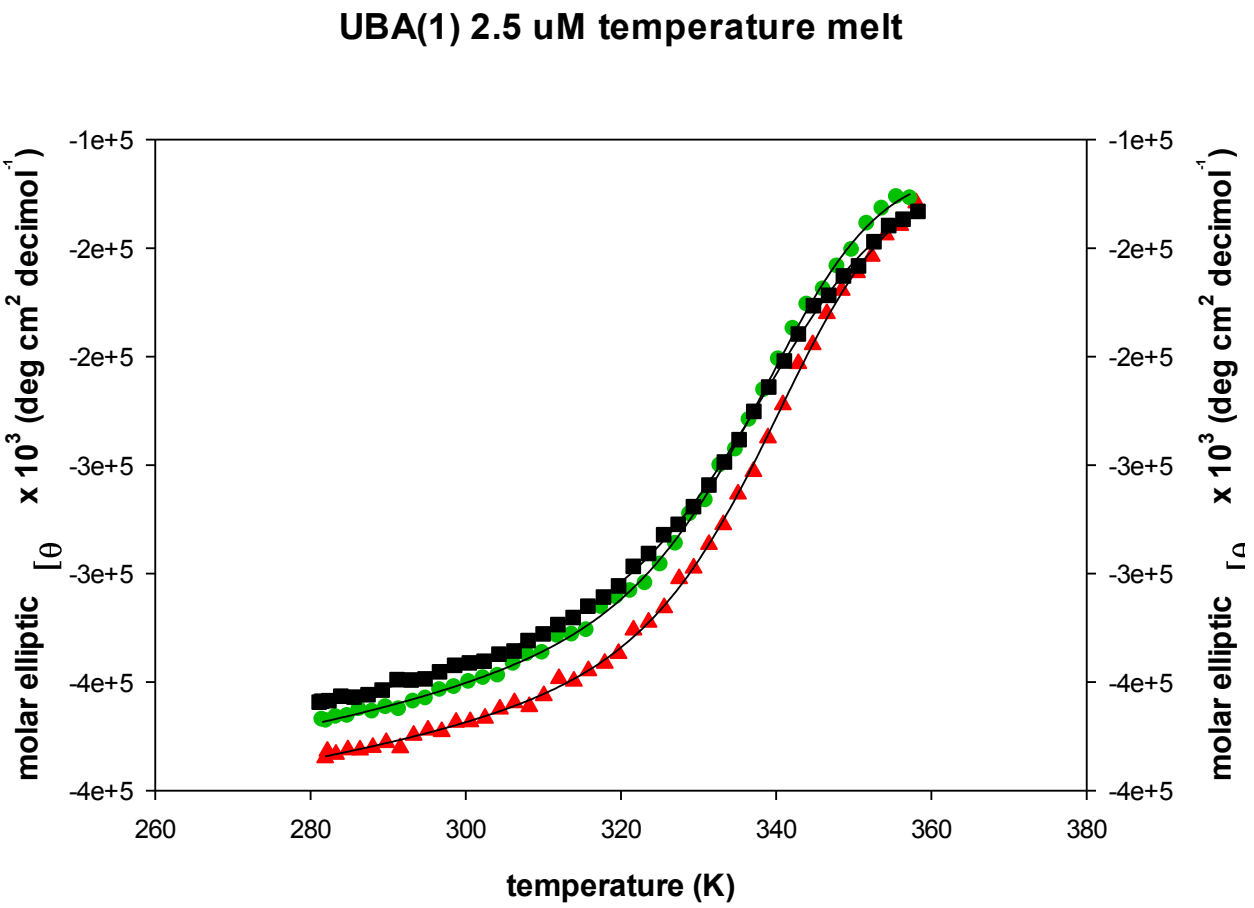

Fig. 3.15. 2.5 uM HHR23A UBA(1) domain melting profiles showing three trials and their respective non-linear least squares fits to the Gibbs-Helmholtz equation relating free energy as function of temperature

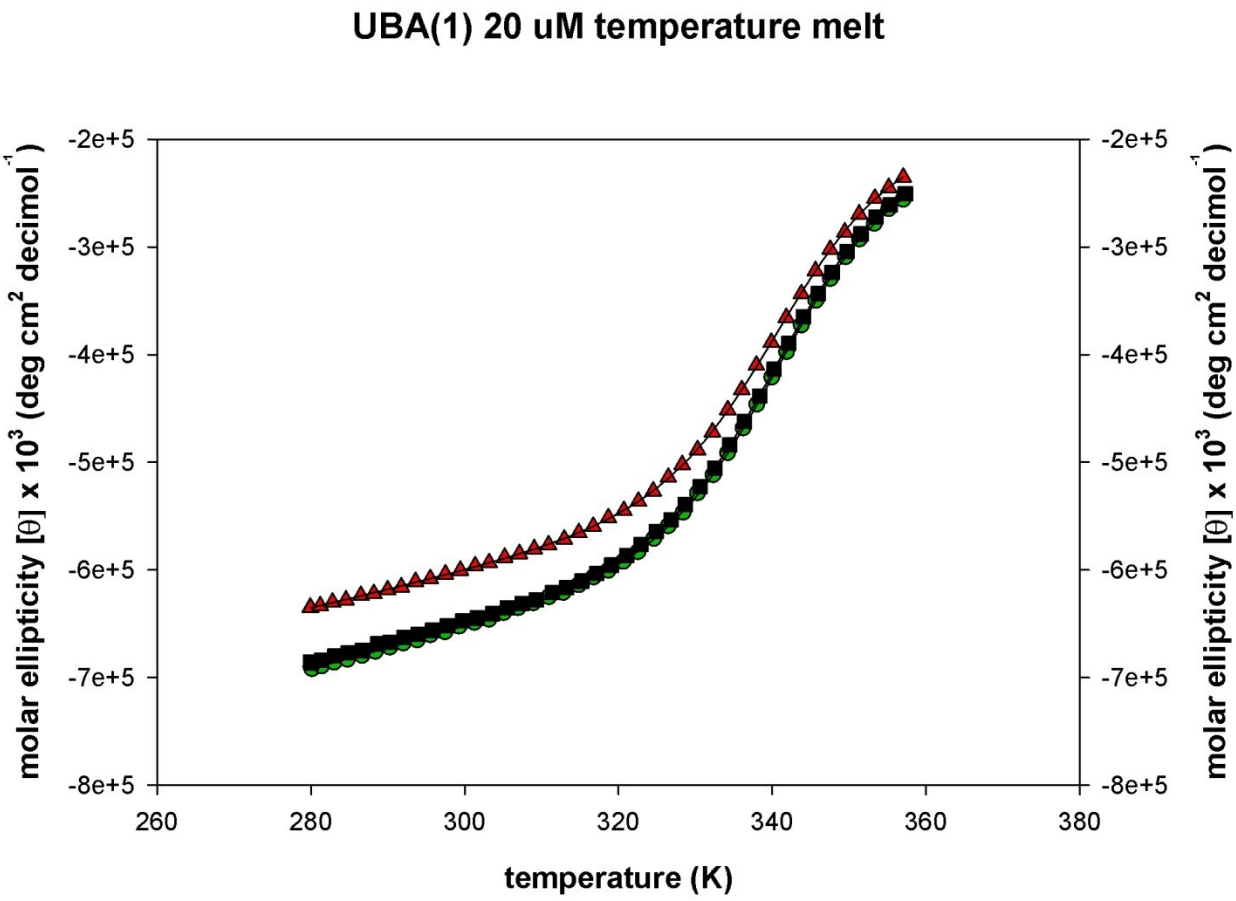

Fig. 3.16. 20 uM HHR23A UBA(1) domain melting profiles showing three trials and their respective fits using non-linear least squares method to the Gibbs-Helmholtz equation examining free energy as function of temperature.

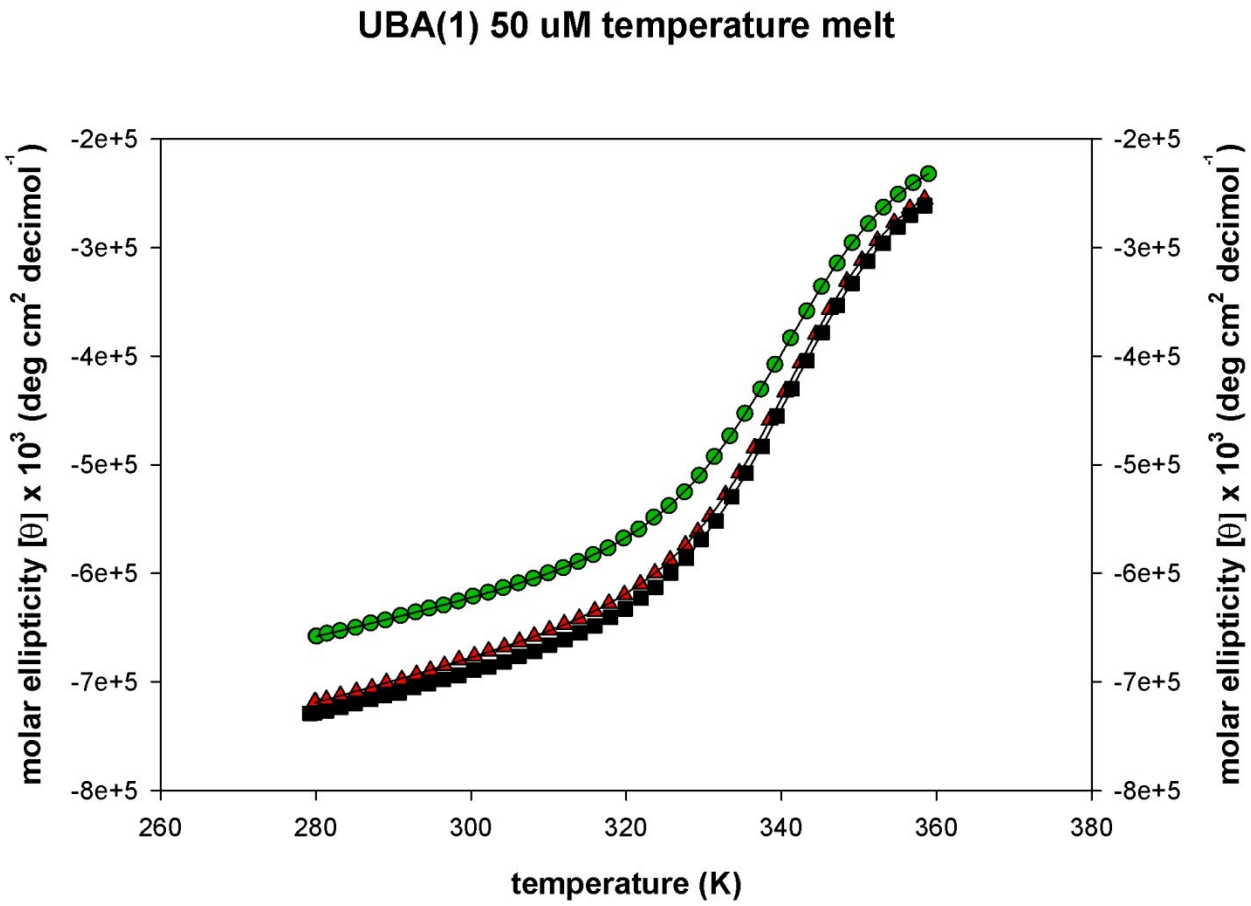

Fig. 3.17. 50 uM HHR23A UBA(1) domain melting profiles showing four trials and their respective fits using non-linear least squares methods to the Gibbs-Helmholtz equation examining free energy as function of temperature.

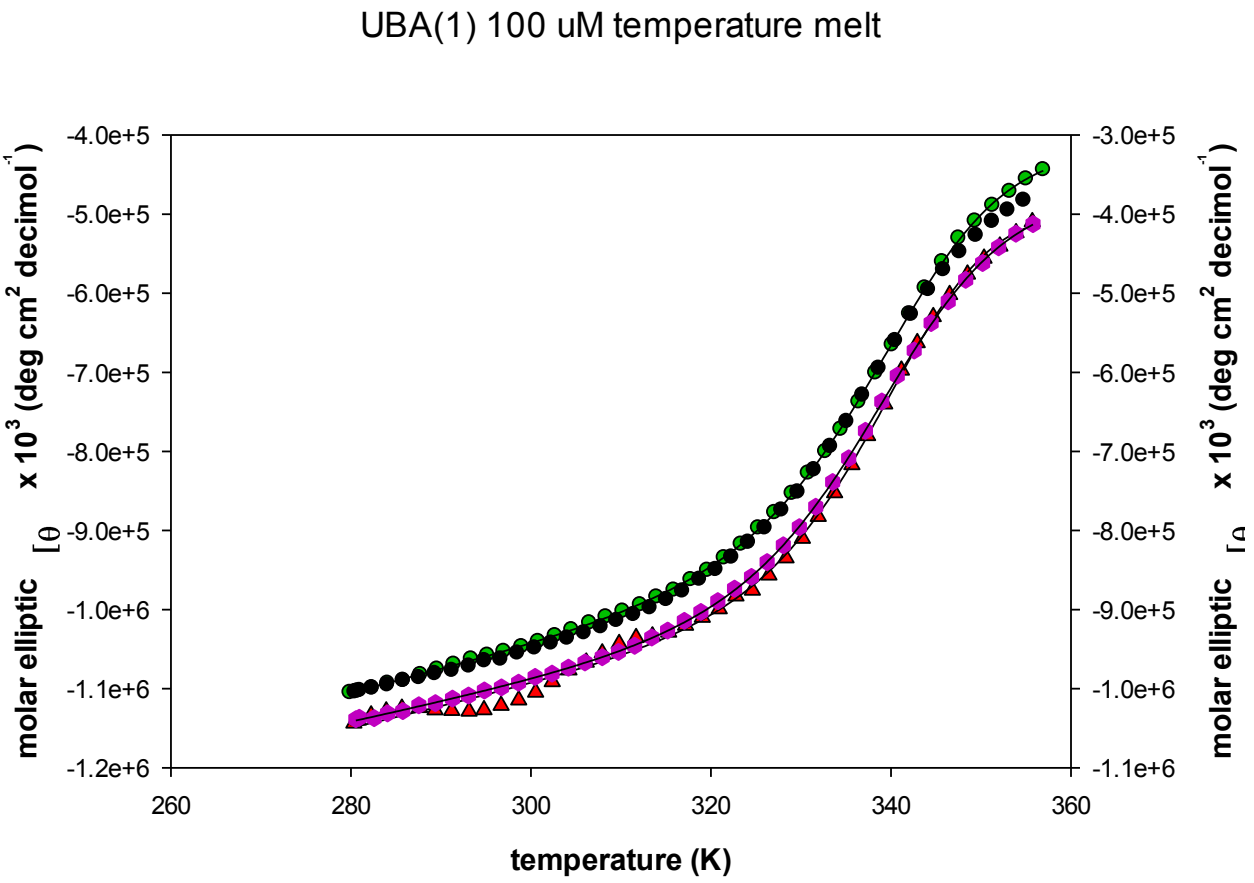

Fig. 3.18. 100 uM HHR23A UBA(1) domain melting profiles showing four trials and their respective fits using non-linear least squares methods to the Gibbs-Helmholtz equation examining free energy as function of temperature.

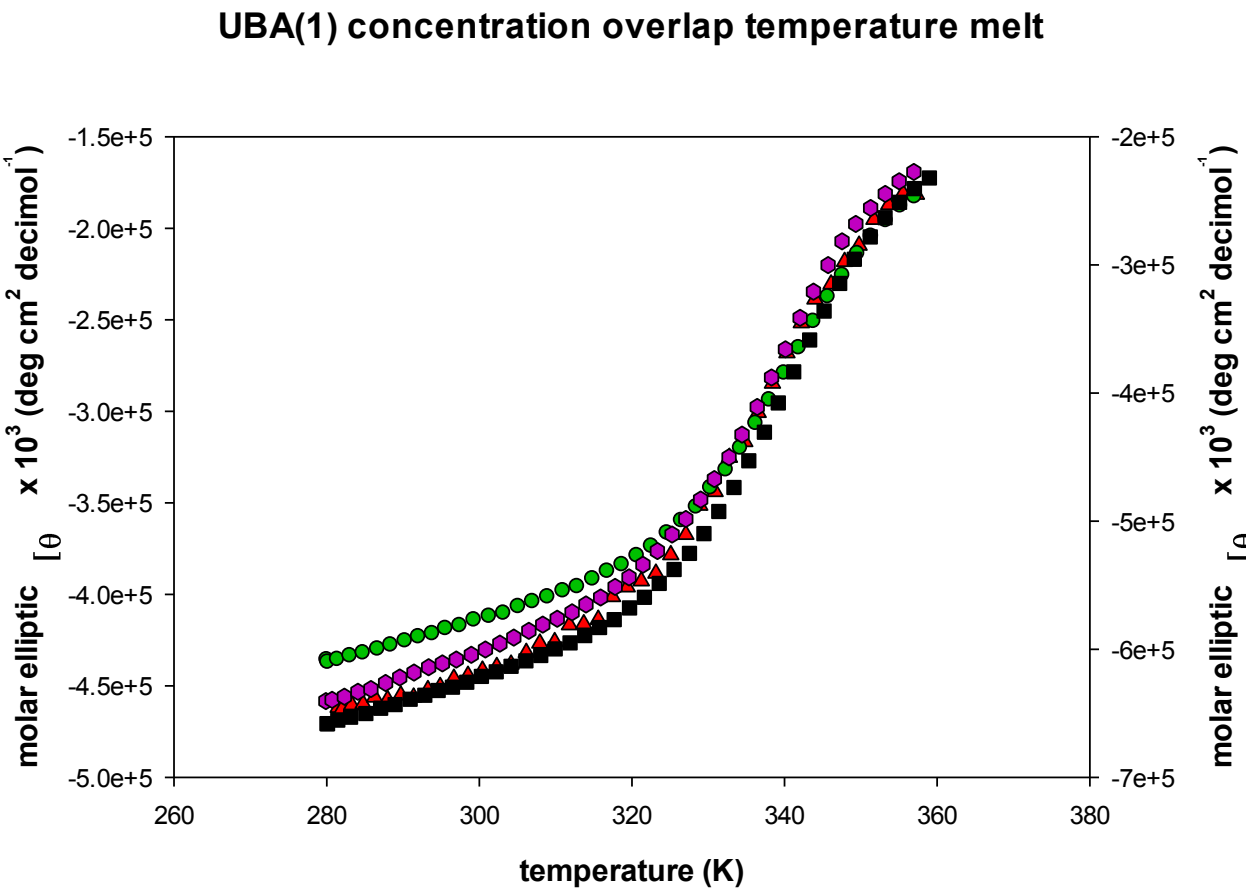

Fig. 3.19. Sample overlay of each of melting curve at different HHR23A UBA(1) domain concentrations (2.5 uM = red, 20 uM = green, 50 uM = black, 100 uM = purple) showing consistent trends in the melting profiles; y-axis adjusted for differences in molar ellipticity at 222 nm.

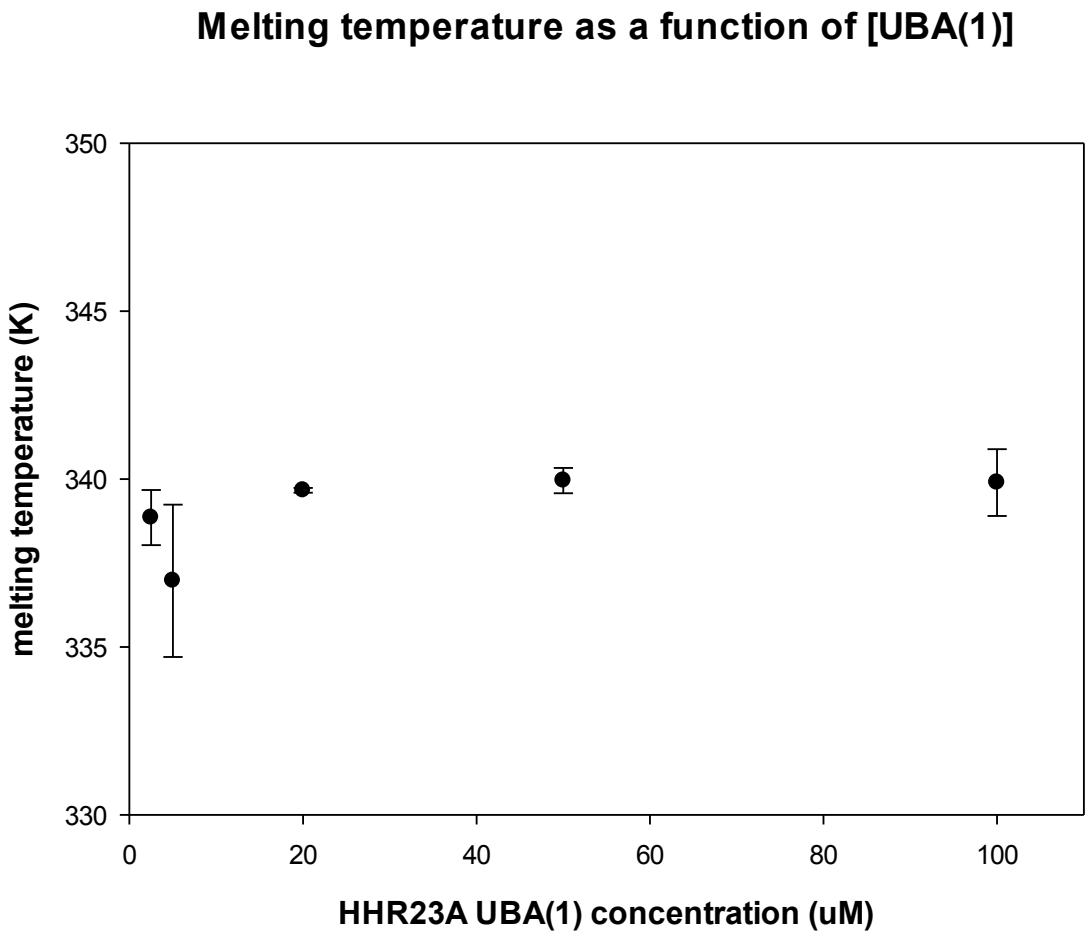

Fig. 3.20. Melting temperature as a function of UBA(1) domain concentration depicting little change in the T_m from 2.5 – 100 uM concentration

Thermodynamic parameter	UBA(1) 2.5 uM	UBA(1) 5 uM	UBA(1) 20 uM	UBA(1) 50 uM	UBA(1) 100 uM
H_m (kcal/mol)	26.1 ± 1.5	28.5 ± 1.6	31.5 ± 0.4	31.1 ± 0.64	31.4 ± 1.9
ΔG_u (298.15 K)	1.99	2.23	2.68	2.62	2.66
T_m (K)	339 ± 0.82	337 ± 2.3	340 ± 0.07	340 ± 0.40	340 ± 1.0

Table 3.2. Thermodynamics of temperature unfolding for the HHR23A UBA(1) domain. Data shows free energy of unfolding at 298.15 K and consistency for the melting temperature (2.5 – 100 uM) indicating no change in the stability of this domain and no dimerization.

Chapter 4: Discussion, Conclusions, and Future Directions

Because protein folding studies are dependent on a single molecule, it was important to determine whether the HHR23A UBA(1) domain exhibits quaternary structure. The thermal denaturation studies using 2.5, 5, 20, 50, and 100 uM HHR23A UBA(1) domain concentrations suggest there is no quaternary structure occurring in this range. If UBA(1) had quaternary structure, there would be a substantial shift in the melting temperature (T_m), indicating a shift in the equilibrium constant for unfolding, K_u, because of stabilization of the folded state by dimerization. Applying the Gibbs-Helmholtz thermodynamic equation to determine the changes of Gibbs free energy as a function of temperature, we see no significant change in the melting temperature or the unfolding enthalpy of the UBA(1) domain over a broad protein concentration range.

The UBA(1) guanidine hydrochloride melting study carried out at 298.15 K yields a free energy of unfolding (ΔG_u = 2.98 kcal/mol) that is similar to the UBA(1) ΔG_u from heat denaturation extrapolated to 298.15 K, regardless of UBA(1) protein concentration used (ΔG_u = 2.7 kcal/mol, see Table 3.2). Jed Long and colleagues discovered using thermal denaturation via far UV circular dichroism that their p62 UBA domain demonstrated a shift in the T_m around 10 uM. The melting temperature below 10 uM was approximately 340 K, while at concentrations of 10 uM and higher the melting temperature of the p62 UBA domain shifted to approximately 345 K. Our melting temperature data at 5 uM HHR23A UBA(1) concentration indicated a value of about 337 K; however, we carried out a thermal melt experiment at 2.5 uM HHR23A UBA(1) concentration, and the T_m value of 339 K corresponded well to the T_m values at higher concentrations of the HHR23A UBA(1) domain (Table 3.2) .

Jed Long et. al. also carried out isothermal titration calorimetry studies to determine a equilibrium dissociation constant and were able to fit a K_d of approximately 6 uM. We carried

out an isothermal titration calorimetry experiment with about 1 mM UBA(1) titrated into UBA pH 6.5 buffer; however, we were unable to fit this data because of signal to noise issues with the MicroCal VP-ITC instrumentation. Furthermore, we did carry out a dissociation equilibrium experiment using Nanotemper microscale thermophoresis (monolith instrumentation using fluorophore at the N-terminus of UBA(1)) to determine whether there was UBA(1) self-association, and discovered a K_d of ~ 6 uM (Appendix, Fig. 5.1). This experiment was replicated only once however, and our other data which is more reliable suggests this is not occurring.

Moreover, size exclusion chromatography replications of the HHR23A UBA(1) domain at different concentrations (600 uM, 100 uM, 50 uM) give nice overlays revealing similar elution volumes, implying that even at concentrations greater than 100 uM, no dimerization evidence is observed for HHR23A UBA(1) domain, at least until 600 uM, which would agree with Juli Feigon's NMR line broadening data. In addition, native polyacrylamide gel electrophoresis using a UBA(1) concentration of 30 uM indicates one Coomassie blue stained band at approximately 5.6 kD (insulin used as a standard), which implies UBA(1) is monomeric at this concentration.

The denaturing conditions of the matrix could explain why both HHR23A UBA domains show dimerization (Figs. 3.1, 3.2). Because size exclusion chromatography of the UBA(1) and the UBA(2) C26A domain elute at their monomeric molecular weights, it is reasonable to suggest that the UBA(2) C26A domains does not form quaternary structure with itself.

Interestingly, the HHR23A UBA(1) domain interacts with bovine ubiquitin as shown using size exclusion chromatography (Figs 3.5). The kinetics, at least qualitatively, seem to be slow with this process, as a 5 minute incubation time with equimolar amounts of the UBA(1) domain with bovine ubiquitin was inadequate for a shift in the elution volume. However, a

change in the elution volume was observed when this domain was individually mixed in equimolar amounts with bovine ubiquitin for 25 minutes.

Therefore, we conclude from our data that quaternary structure is not occurring for the HHR23A UBA(1) domain, and more likely than not, also not occurring for the UBA(2) C26A domain. However, additional robust methods need to be applied to the UBA(2) C26A domain to assess whether this is occurring.

For future directions, the kinetics of the UBA(1) domain need to be carried out to ascertain rate constants for its folding pathway. Briefly, tyrosine fluorescence using stopped-flow kinetics will be used to determine these rate constants under strong denaturing conditions. In addition, the thermodynamics of three helix bundles (UBA domains) extend to work using a cytochrome *c* – UBA(2) plasmid construct. Our lab has a cytochrome *c* - UBA(2) domain construct where the C26A mutation has been successfully inserted. The cytochrome *c* – UBA(2) C26A guanidine melt reveals the presence of an intermediate (Fig. 4.1). The proposed experiments on this protein are to engineer histidine mutations in the UBA(2) C26A portion of cytochrome *c* – UBA(2) C26A fusion protein and to determine the loop formation thermodynamics under denaturing conditions. This is important to determine, as data in our lab has discovered that foldable sequences behave differently from homogenous peptide sequences (K. Sudhindra Rao, 2009). This suggests large variations in the foldable sequence backbone conformations.

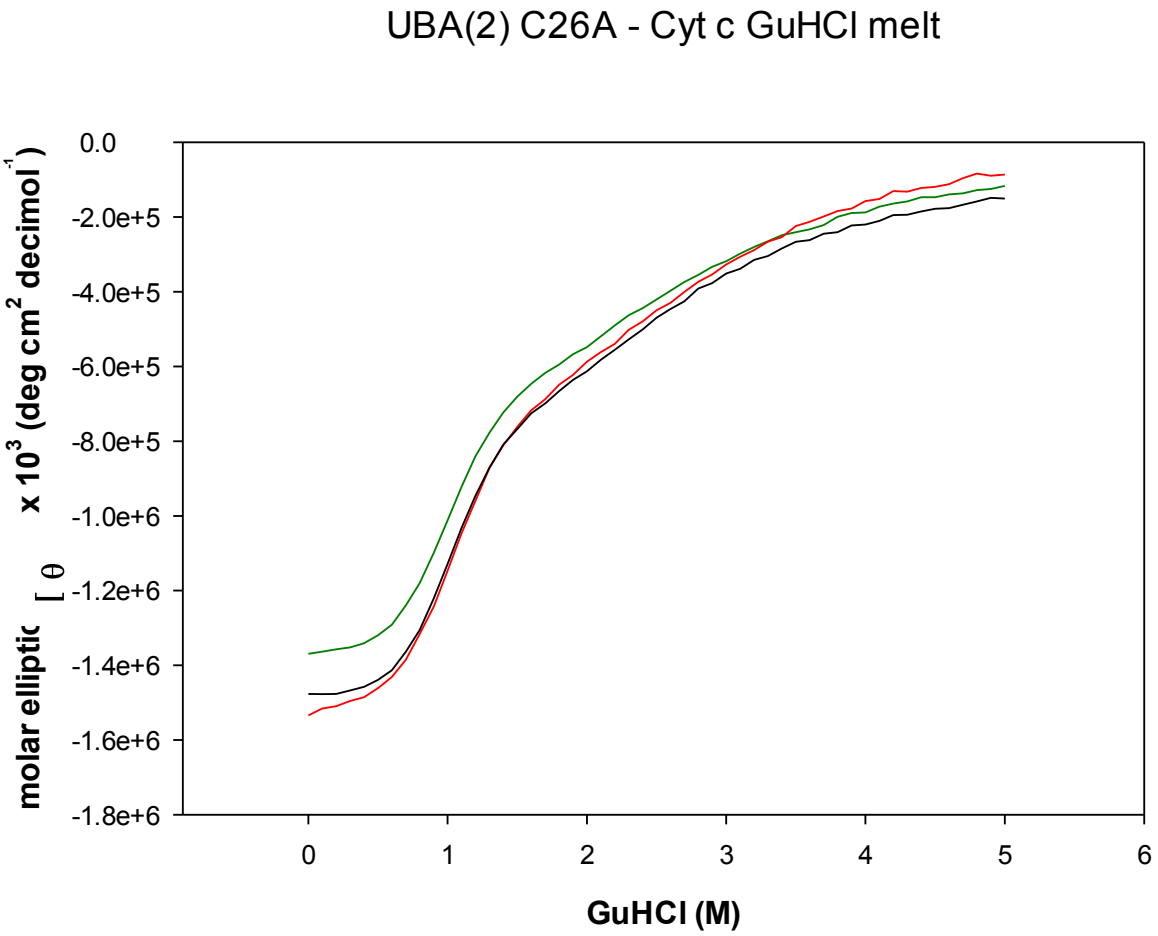

Fig. 4.1. Guanidine hydrochloride titration melt of UBA(2) C26A – cytochrome *c* showing unfolding of cytochrome *c* followed by unfolding of the HHR23A UBA(2) C26A domain. Data shows presence of an intermediate, which can be fit to a 3-state GuHCl model to determine the Gibbs free energy of unfolding.

Appendix

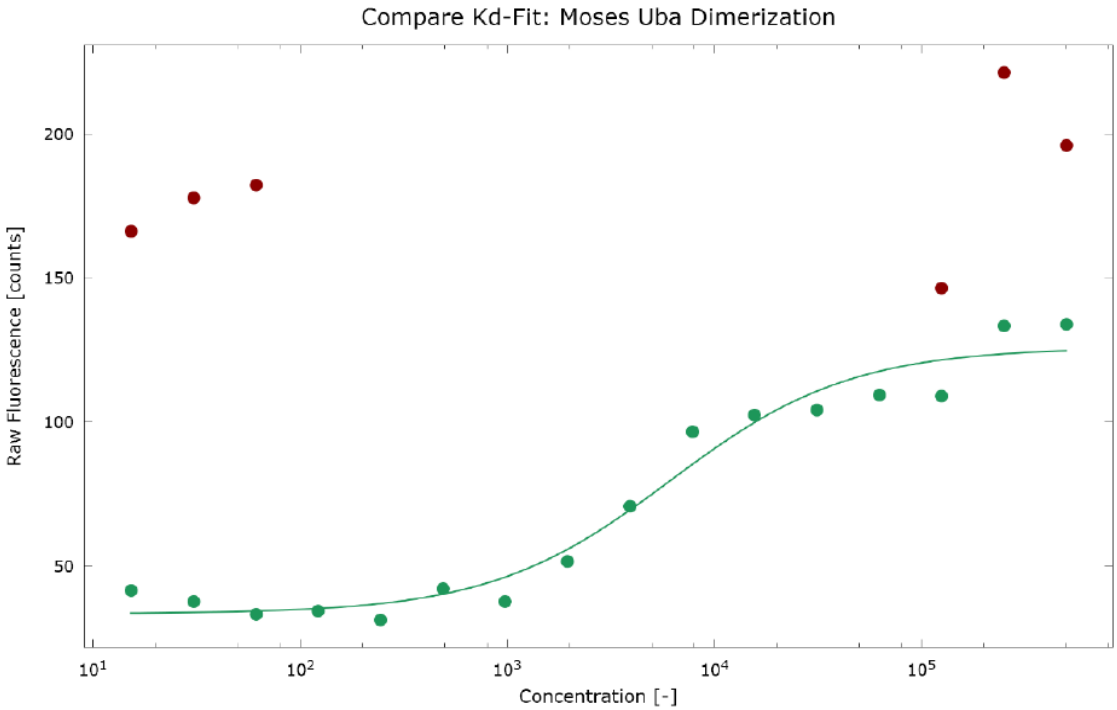

Fig. 5.1. For performing experiments with the Uba protein, a fluorescent label (NT-647) was covalently attached to the protein (NHS coupling). In the MST experiment we have kept the concentration of NT-647 labeled Uba constant, while the concentration of the non-labeled Uba was varied between 500 µM – 15.3 nM. The assay was performed in buffer provided by the experimenter. After a short incubation the samples were loaded into MST NT.115 premium glass capillaries and the MST analysis was performed using the Monolith NT.115. Concentrations on the x-axis are plotted in nM. A *Kd* of **6.1 µM +/- 1.6 µM** was determined for this interaction.

Please note: The interaction of Uba with the NT-647 labelled Uba was a homodimerization experiment, with a serial dilution of Uba performed against a constant concentration of NT-647 labelled Uba that is less than the homodimerization affinity. The interaction of Uba with the NT-647 labelled Uba resulted in a dose dependent shift in the raw fluorescence intensity of the NT-647 labelled Uba, so the *Kd* for the homodimerization affinity was determined by analyzing the raw fluorescence (green dots). A control experiment was performed wherein the samples were denatured with SDS and DTT, which eliminated the dose dependent shift in the raw fluorescence (red dots). The elimination of the shift in NT-647 labelled Uba raw fluorescence upon sample denaturation confirmed that the raw fluorescence shift was caused by the homodimerization.

References

Anfinsen, Christian B. (1973). Principles that Govern the Folding of Protein Chains. *Science, 181*(4096), 223-230.

Burcu Anil, Benben Song, Yuefeng Tang, Daniel P. Raleigh;. (2004). Exploiting the Right Side of the Ramachandran Plot: Substitution of Glycines by D-Alanine Can Significantly Increase Protein Stability. *J. AM. CHEM. SOC., 126*, 13194-13195.

Ginka S. Buchner, Natalie Shih, Amy E. Reece, Stephan Niebling, Jan Kubelka. (2012). Unusual Cold Denaturation of a Small Protein Domain. *Biochemistry, 51*, 6496-6498.

Gregersen N, Bross P. (2010). Protein misfolding and cellular stress: an overview. *Methods Mol Bio, 648*, 3-23.

Jed Long, Thomas P. Garner, Maya J. Pandya, C. Jeremy Craven, Ping Chen, Barry Shaw, Michael P. Williamson, Robert Layfield, Mark S. Searle. (2010). Dimerisation of the UBA Domain of p62 Inhibits Ubiquitin Binding and Regulates NF-kB Signalling. *J. Mol. Biol., 396*, 178-194.

K. Sudhindra Rao, Franco O. Tzul, Arwen K. Christian, Tia N. Gordon, Bruce E. Bowler. (2009). Thermodynamics of Loop Formation in the Denatured State of Rhodopseudomonas palustris Cytochrome c': Scaling Exponents and the Reconcilation Problem. *J. Mol. Biol., 392*(5), 1315-1325.

Margoliash, E.; Frohwirt, Nehamah;. (1959, March). Spectrum of Horse-Heart Cytochrome c. *Biochem J., 71*(3), 570-572.

Myers JK, Pace CN, Scholtz JM. (1995). Denaturant m values and heat capacity changes: relation to changes in accessible surface areas of protein folding. *Protein Science, 10*, 2138-2148.

Shin Isogai, Daichi Morimoto, Kyohei Arita, Satoru Unzai, Takeshi Tenno, Jun Hasegawa, Yu-shin Sou, Masaaki Komatsu, Keiji Tanaka, Masahiro Shirakawa, Hidehito Tochio. (2011). Crystal Structure of the Ubiquitin-associated (UBA) Domain of p62 and Its Interaction with Ubiquitin. *J. Biol. Chem., 286*, 31864-31874.

Thomas D. Mueller, Juli Feigon. (2002). Solution Structures of UBA Domains Reveal a Conserved Hydrophobic Surface for Protein-Protein Interactions. *J. Mol. Biol., 319*, 1243-1255.

Yoshihisa Hagihara, Saburo Aimoto, Anthony L. Fink, and Yuji Goto. (1993). Guanidine Hydrochloride-induced Folding of Proteins. *J. Mol. Biol., 231*, 180-184.